PCCP

View Online
Dynamic Article Links

Cite this: *Phys. Chem. Chem. Phys.*, 2011, **13**, 10885–10907

www.rsc.org/pccp

PAPER

Practical methods for including torsional anharmonicity in thermochemical calculations on complex molecules: The internal-coordinate multi-structural approximation†

Jingjing Zheng, Tao Yu, Ewa Papajak, I. M. Alecu, Steven L. Mielke and Donald G. Truhlar*

Received 23rd November 2010, Accepted 11th February 2011
DOI: 10.1039/c0cp02644a

Many methods for correcting harmonic partition functions for the presence of torsional motions employ some form of one-dimensional torsional treatment to replace the harmonic contribution of a specific normal mode. However, torsions are often strongly coupled to other degrees of freedom, especially other torsions and low-frequency bending motions, and this coupling can make assigning torsions to specific normal modes problematic. Here, we present a new class of methods, called multi-structural (MS) methods, that circumvents the need for such assignments by instead adjusting the harmonic results by torsional correction factors that are determined using internal coordinates. We present three versions of the MS method: (i) MS-AS based on including all structures (AS), *i.e.*, all conformers generated by internal rotations; (ii) MS-ASCB based on all structures augmented with explicit conformational barrier (CB) information, *i.e.*, including explicit calculations of all barrier heights for internal-rotation barriers between the conformers; and (iii) MS-RS based on including all conformers generated from a reference structure (RS) by independent torsions. In the MS-AS scheme, one has two options for obtaining the local periodicity parameters, one based on consideration of the nearly separable limit and one based on strongly coupled torsions. The latter involves assigning the local periodicities on the basis of Voronoi volumes. The methods are illustrated with calculations for ethanol, 1-butanol, and 1-pentyl radical as well as two one-dimensional torsional potentials. The MS-AS method is particularly interesting because it does not require any information about conformational barriers or about the paths that connect the various structures.

I. Introduction

Torsional motion constitutes an especially challenging form of vibrational anharmonicity for which the harmonic approximation is often highly inaccurate. Furthermore, the presence of multiple torsional degrees of freedom often results in many low-energy conformers that contribute significantly to the partition function. Feynman path integral methods[1,2] provide an accurate and straightforward way to include torsional effects in quantum mechanical partition functions, and while they have already provided important benchmark results for small systems,[3–5] more affordable methods are needed for many applications involving complex molecules.

A variety of separable approximations are available[6–20] that replace the harmonic contribution of specific normal modes by solutions of one-dimensional (1-D) torsional treatments, and nonseparable treatments have also been advanced.[9,14,16,21–25] In many instances torsions are strongly mixed with other torsions and/or with other low-frequency motions such as bending, and in such cases one cannot identify them with specific normal modes. We divide the nonseparable treatments into two classes, those that do not assume a one-to-one correspondence between torsions and individual normal modes, and those that do; we call these mixed torsion models and normal mode substitution models. The only widely discussed model that allows mixed torsions is the Pitzer–Gwinn approximation.[21] This requires evaluating the full-dimensional classical configuration integral,[26] which—although less expensive than a path integral—is still too expensive for routine use on large molecules because it requires either extensive Monte Carlo sampling by direct dynamics (electronic structure calculations on the fly) or the careful fitting of an analytic nonseparable potential function. Reduced-dimensional path integrals[23,27–29] and classical configuration integrals covering only torsional degrees of freedom[9,16] have also been considered

Department of Chemistry and Supercomputing Institute, University of Minnesota, Minneapolis, MN 55455-0431. E-mail: truhlar@umn.edu
† Electronic supplementary information (ESI) available: Partition functions, standard state entropies, and coordinates of optimized structures. See DOI: 10.1039/c0cp02644a

but are more expensive than the methods to be proposed here. On the other hand, methods employing normal mode substitution[7–10,12–14,22] are not general enough for our purpose.

In this article we will consider a family of new torsional approximations that employ internal-coordinate correction factors to the harmonic treatment that avoid not only the separability assumption but also the restriction associated with assigning torsions to specific normal modes.

In many cases, the thermochemical properties of a chemical substance can be reasonably estimated by using the group additivity method—the assumption that the thermodynamic properties of a given species can be obtained by summing the contributions from each group comprising that species. The most widely employed version of group additivity was formulated by Benson,[30] and established general group additivity values through a two-step process involving first compartmentalizing similar molecules with known thermodynamic properties into their constituent groups—where a group is defined as a polyvalent atom and all of its ligands—and then deriving the contribution to various thermodynamic properties due to each group through multivariable linear regression fits to the available experimental data.[30] The original group additivity values established by Benson for stable molecules were later adapted to several classes of free radical species by O'Neal and Benson,[31,32] and were subsequently updated by Cohen[33] to account for new experimental and theoretical findings. More recently, Lay *et al.*[34] developed an alternative technique for estimating bulk thermodynamic properties, often with improved accuracy, from a single group called the H atom bond increment (HBI) group. We used these various group additivity techniques to estimate the entropies of the species studied in this work and compare them to our methods.

For the convenience of the reader, we use a consistent set of acronyms for frequently repeated phrases and methods. A glossary of these acronyms is provided in Appendix A.

II. Theory

II. A Overview

The most direct consequence of internal rotation is the occurrence of multiple conformational minima. A conventional approach[35,36] to calculating partition functions in such cases is to use the harmonic approximation for the minimum-energy structure and to replace contributions from certain normal modes with a hindered rotor treatment by using the tables of Pitzer and Gwinn[21] or an analytic hindered rotor,[7,10] or free rotor approximation. A somewhat more complicated case occurs when a torsion is unsymmetrical (or isotopically substituted) so that the minima encountered along the torsion are distinguishable. Then, if one assumes that the vibrational modes are separable, the partition function for each of the unsymmetrical torsional motions has contributions from each distinguishable conformer. However the treatment of torsions as separable can be very unrealistic.[12,37–41] A better approach is to start with a list of distinguishable structures (*i.e.*, distinguishable conformers) and to sum their contributions, including at least torsional anharmonicity. We call such methods multi-structural (MS) approximations, and these are the subjects of the present paper.

II. B MS-AS method

II.B.1 Theory for nearly separable torsions. Let Q denote a multidimensional partition function and q denote the partition function for a single degree of freedom. In the convention used in this article, all partition functions have their zero of energy at their local minimum (rather than being normalized to unity at 0 K). We will consider J distinguishable structures, *i.e.*, conformational minima, $j = 1, 2,\ldots,J$, and we will include anharmonicity in several torsions labeled $\tau = 1, 2,\ldots,t$; we note that t has the same value for all structures. Let the energies of the minima be U_j where U_1 has a value of zero, and all other U_j are positive. We divide the t torsions into two types: nearly separable (NS) and strongly coupled (SC). For NS torsions, we may define a parameter $M_{j,\tau}$ to be the total number of minima, whether distinguishable or not, along torsional coordinate τ of structure j (each of these minima correspond to another structure).

In our initial presentation we shall focus on the special case that all the torsions are nearly separable and we will further assume that the $M_{j,\tau}$ minima may be reasonably approximated as being evenly distributed along the torsional coordinate τ. In section II.B.2 we will present an alternative derivation of the MS-AS approximation based on a different rationale for assigning the $M_{j,\tau}$ parameters and that may be useful in more general contexts, including some cases of strong coupling between the torsions. The alternative derivation explicitly accounts for cases where the minima are not approximately evenly distributed along a given torsional coordinate. In section II.C we will present a variation of the multi-structural method that utilizes explicit barrier information instead of the $M_{j,\tau}$ parameters, and in section II.D we will consider a variation of the method designed to treat the most challenging cases of strong coupling wherein parameters are obtained by Voronoi tessellation.[42–44] In general we can use a hybrid scheme for obtaining $M_{j,\tau}$; for example, we use the notation NS : SC = n : m to denote that n torsions are treated as nearly separable and m torsions are treated as strongly coupled. In this language, the present section (II.B.1) is devoted to the case t : 0.

We will denote the torsional symmetry numbers as σ_τ and the number of distinguishable minima for torsional coordinate τ of structure j as $P_{j,\tau}$ where

$$P_{j,\tau} = M_{j,\tau}/\sigma_\tau. \quad (1)$$

The symmetry numbers σ_τ can be determined by treating the least symmetric of the two rotating fragments as a fixed frame and counting the number of identical structures obtained when the more symmetrical top is rotated from 0 to 360 degrees and relaxed (for example, the symmetry numbers for methanol, nitromethane, and 1,2 dichloroethane are 3, 3, and 1, respectively). Once all the structures are found, the number, $P_{j,\tau}$, of unique structures connected to structure j (including itself) by internal rotation τ may often be identified by counting the structures that have similar torsion angles for all other internal rotations; when strong torsional coupling

exists additional considerations may be necessary as will be discussed further below. Attempts have been made[12,45] to fully automate the assignment of the $P_{j,\tau}$ (or equivalently the $M_{j,\tau}$), but such approaches are beyond the scope of the present study.

In general, the internal moment of inertia, $I_{j,\tau}$, associated with rotation about a specific axis τ is a continuous function of geometry, but we will approximate it as a constant within the domain of each specific structure and will assign values $I_{j,\tau}$ that are calculated for rotation about the bond axis associated with torsion τ at the minimum-energy geometry of structure j using the method of Pitzer.[46] (In previous articles,[13,14] we denoted Pitzer's method for calculating the internal moment of inertia for an internal rotation as the curvilinear method, abbreviated C.) Pitzer[46] has pointed out that the geometry dependence of the moments of inertia approximately compensates for the change in the product of the vibrational frequencies as a function of the internal rotation angle. This justifies holding the internal moments of inertia fixed at their values at the minimum-energy geometry when the vibrational motions are approximated by a classical harmonic treatment; however, we include quantum effects, and we use this approximation even when the classical harmonic approximation is not valid.

Pitzer's method[46] for calculating internal moments of inertia assumes that all molecular fragments that undergo internal rotation are attached to a unique fixed frame; for cases with more than one torsion the scheme is approximate unless a determinant-based approach is used to fully account for intermode coupling. A more-general treatment is available in the work of Kilpatrick and Pitzer[47] that accounts for the coupling between torsional motions and removes the requirement of a unique fixed frame. In the following, when we refer to Pitzer moments we are referring to moments calculated in the absence of intermode coupling; approaches that include intermode coupling have only rarely been employed in earlier work, but here, in addition to the uncoupled Pitzer moments, we also employ the general treatment of Kilpatrick and Pitzer.[47] The Kilpatrick and Pitzer[47] treatment leads to the calculation of a kinetic energy matrix for internal rotation denoted as **D** (alternatively one may work with the kinetic energy matrix **S** associated with overall rotation and internal rotation) which may be diagonalized to yield moments associated with linear combinations of coupled torsions. The moments of Pitzer[46] are the diagonal elements of the **D** matrix and in the limit of weak torsional coupling (where **D** is strongly diagonally dominant) torsional motion is well represented by rotation about a single bond. Our torsional approximation scheme begins by approximating torsional motions as being uncoupled within the domain of a specific structure so we begin by employing the approximate Pitzer moments. However, in the high-temperature limit the partition function scales as the square root of the determinant of **D**, and we gradually switch to the Kilpatrick–Pitzer coupled moments as the temperature is increased.

The torsional coordinate associated with the Pitzer internal moments of inertia describes the rotation of a rigid top against a fixed frame, and various considerations have been used to define physical torsion coordinates for flexible systems.[48–50] In our internal-coordinate treatment, we approximate the torsional coordinate by a single dihedral angle. Thus, our torsional force constants and other results have a small dependence on the choice of coordinate system, *i.e.*, on which dihedral angle we choose. One consequence of using internal coordinate torsion angles is that subtle deviations from expected symmetries may be observed; for example, methyl groups may deviate very slightly from the expected three-fold symmetry. In such cases we use values of $M_{j,\tau}$, $P_{j,\tau}$, and σ_τ that would have been obtained from the more symmetrical structures. All of the methods presented here assume that the domains of different conformers do not significantly overlap; in cases where slight symmetry lowering leads to strongly overlapping structures it may be best to include only one of the strongly overlapping structures and treat this conformer using a symmetry number that would have been appropriate in the absence of symmetry lowering.

If there is only one conformer and we neglect coupling between electronic, vibrational, and rotational degrees of freedom, the total partition function of a system can be written as

$$Q_{\text{total}} = Q_{trans} Q_{\text{elec}} Q_{\text{rot}} \prod_{m=1}^{F} q_{\text{vib},m} \tag{2a}$$

where Q_{trans} is the translational partition function, Q_{elec} is the electronic partition function, Q_{rot} is the rotational partition function, $F = 3N - 6$ for a nonlinear molecule (where N is number of atoms in the system), and $q_{\text{vib},m}$ is the vibrational partition function of mode m. However, we do not use that simplification; instead, we write

$$Q_{\text{total}} = Q_{trans} Q_{\text{elec}} Q_{\text{con-rovib}} \tag{2b}$$

where $Q_{\text{con-rovib}}$ is the conformational-rovibrational partition function. In this article, the translational and electronic partition functions are not discussed. We mainly focus on the vibrational partition function, but eqn (2b) also allows for a conformational average and for the change of rotational partition function from structure to structure. Thus, we do not assume that rotation is separable in an overall sense because the rotational partition function depends on the structure.

Special consideration is needed with considering symmetry numbers for systems with internal rotations. The overall torsional symmetry number associated with the torsion-only degrees of freedom is

$$\sigma_{\text{torsion}} = \prod_{\tau=1}^{t} \sigma_\tau \tag{3}$$

and is the same for all structures. However, the structures can include cases both with and without rotational symmetry so that the rotational symmetry numbers $\sigma_{\text{rot},j}$ depends on j. It should be realized that the rotational symmetry elements that transform symmetrical structures into themselves transform unsymmetrical structures into *other* unsymmetrical structures that appear in the list of the J structures that are distinguishable when only considering torsional symmetry, and therefore $\sigma_{\text{rot},j}$ depends on how these structures are treated. We can make this clear by an example. Consider pentane,[51] which has 11 torsional conformers; eight of these structures have no rotational symmetry and thus have $\sigma_{\text{rot},j}$ equal to 1, whereas

three of them have $\sigma_{\mathrm{rot},j} = 2$. Of the eight structures with $\sigma_{\mathrm{rot},j} = 1$, only four are distinguishable when rotation is considered because each structure may be transformed into one other structure by an overall rotation. Thus, if all eleven structures are included in the MS-AS partition function calculations each of the rotational partition functions should use a symmetry number of 2. Alternatively, one could include only the seven structures that are distinguishable after considering both rotational and torsional symmetries, in which case the rotational partition functions would use the structure-dependent $\sigma_{\mathrm{rot},j}$ values.

We propose a new family of approximations to be called multi-structural methods. The first member of the family is the MS-AS method in which we include all structures. The conformational-rovibrational partition function is given in the MS-AS method by

$$Q_{\mathrm{con\text{-}rovib}}^{\mathrm{MS\text{-}AS}} = \sum_{j=1}^{J} Q_{\mathrm{rot},j} \exp(-\beta U_j) Q_j^{\mathrm{HO}} Z_j \prod_{\tau=1}^{t} f_{j,\tau} \qquad (4)$$

where $Q_{\mathrm{rot},j}$ is the rotational partition function of structure j (here we use the classical approximation for rotational partition functions, see eqn (B4)), β is $1/k_{\mathrm{B}}T$ where k_{B} is Boltzmann's constant and T is temperature, Q_j^{HO} is the usual normal-mode harmonic oscillator vibrational partition function calculated at structure j, Z_j is a factor (specified below) designed to ensure that the MS-AS scheme reaches the correct high-T limit (within the parameters of the model), and $f_{j,\tau}$ is an internal-coordinate torsional anharmonicity function that, in conjunction with Z_j, adjusts the harmonic result of structure j for the presence of the torsional motion associated with coordinate τ.

We use MS-HO to denote the partition function calculated without Z_j and $f_{j,\tau}$, that is, with all Z_j and all $f_{j,\tau}$ equal to unity. One can use normal-mode analysis to obtain frequencies to calculate Q_j^{HO}. A key advantage of eqn (4) over the MS-HO approximation is that it includes torsional anharmonicity, but it is not necessary to assign each torsional motion to a specific normal mode. The MS-HO approximation is already an improvement over treatments that include only the lowest-energy conformation, and the importance of including a conformational average when computing enthalpies has recently been emphasized.[36,52]

We define the torsional correction functions $f_{j,\tau}$ as the ratio of a partition function for some accurate method to treat a given torsion divided by a harmonic partition function for a frequency $\bar{\omega}_{j,\tau}$, where the frequency $\bar{\omega}_{j,\tau}$ is defined as the harmonic frequency obtained using internal coordinates rather than a normal-coordinate frequency. This scheme avoids identifying each torsional mode with a specific normal mode. The internal-coordinate torsional frequency is obtained by

$$\bar{\omega}_{j,\tau} = \sqrt{\frac{k_{j,\tau}}{I_{j,\tau}}} \qquad (5)$$

$$k_{j,\tau} \equiv \left.\frac{\partial^2 V}{\partial \phi_\tau^2}\right|_{\phi_\tau = \phi_{\tau,\mathrm{eq,j}}} \qquad (6)$$

where $k_{j,\tau}$ is the force constant of a specific torsion τ at structure j, V is the potential energy, and the torsion τ is represented by a dihedral angle ϕ_τ whose equilibrium value is $\phi_{\tau,\mathrm{eq},j}$.

The internal-coordinate force constants can be calculated either by numerical finite differences or by transforming force constant matrices expressed in Cartesian coordinates into force constant matrices in non-redundant internal coordinates.[53–58] In the numerical finite difference method, one rotates one of the two tops with respect to the other by a small amount and uses central differences to calculate the second derivative from the equilibrium energy and single-point energies of the two slightly distorted geometries. In the transformation method, one has to be careful to select an appropriate set of $3N - 6$ independent internal coordinates. The strategy we employ to select the $3N - 6$ independent internal coordinates is that (i) all bond stretching coordinates are included, (ii) only one dihedral angle is selected for each torsional mode, and (iii) the rest of the coordinates are bond angles and other dihedral angles not related to torsions (*e.g.*, dihedral angles for out-of-plane motion in a ring structure) that are selected while avoiding redundant choices. By using such a set of $3N - 6$ independent internal coordinates, the second partial derivative of V with respect to the dihedral angle is the force constant for this torsion. In this paper, all the torsional force constants are calculated by the transformation method.

The reference Pitzer–Gwinn (RPG) method[14,21] denotes the use of a one-dimensional Pitzer–Gwinn approximation applied to a reference potential (rather than the true potential as in the Pitzer–Gwinn method) where the reference potential is obtained from limited information. The reference potential was previously taken as[7,14,21,46]

$$V_m = \frac{W_m}{2}[1 - \cos(M_m \phi_m)] \qquad (7)$$

where V_m is the potential of normal mode m, ϕ_m is a torsion coordinate, M_m is the number of minima in mode m, and W_m is a torsional barrier height. If all the torsional barriers do not have the same height, W_m would be an effective or average height. Here we instead use

$$V_{j,\tau} = U_j + \frac{W_{j,\tau}}{2}[1 - \cos M_{j,\tau}(\phi_\tau - \phi_{\tau,\mathrm{eq},j})]; \quad \frac{-\pi}{M_{j,\tau}} \le \phi_\tau - \phi_{\tau,\mathrm{eq},j} \le \frac{\pi}{M_{j,\tau}} \qquad (8)$$

where $W_{j,\tau}$ is an effective barrier height associated with structure j. When the RPG method is applied to eqn (8), $f_{j,\tau}$ can be written as

$$f_{j,\tau} = \sigma_\tau \left[\frac{q_{j,\tau}^{\mathrm{RC}}}{q_{j,\tau}^{\mathrm{CHO}}}\right] \qquad (9)$$

where $q_{j,\tau}^{\mathrm{CHO}}$ and $q_{j,\tau}^{\mathrm{RC}}$ are the classical harmonic oscillator and reference classical partition functions of the torsion τ for structure j, respectively, given by

$$q_{j,\tau}^{\mathrm{CHO}} = \frac{1}{\hbar\beta\bar{\omega}_{j,\tau}} \qquad (10)$$

and[14]

$$q_{j,\tau}^{\mathrm{RC}} = \frac{1}{M_{j,\tau}} q_{j,\tau}^{\mathrm{FR}} \exp(-\beta W_{j,\tau}/2) I_0(\beta W_{j,\tau}/2) \tag{11}$$

where $\hbar$ is Planck's constant divided by 2π, I_0 is a modified Bessel function, and the free rotor (FR) partition function is given by

$$q_{j,\tau}^{\mathrm{FR}} = \frac{\sqrt{2\pi I_{j,\tau}/\beta}}{\hbar \sigma_\tau} \tag{12}$$

Eqn (7) assumes that all barriers along a torsional coordinate have the same height W_m or at least may be represented by a single average barrier, and that all of the minima have the same energy, whereas eqn (8) provides the flexibility for each structure to have an independent minimum and barrier height. The $W_{j,\tau}$ can be chosen as the average of the barrier heights on either side of this minimum. However, we next make a simplification so that we do not need to know these barriers. The simplification takes advantage of the fact that for a potential of the form of eqn (8) and a geometry-independent internal moment of inertia, the barrier heights, internal moment of inertia, and the torsional frequency are interrelated by[7,14]

$$W_{j,\tau} = \frac{2 I_{j,\tau} \bar{\omega}_{j,\tau}^2}{M_{j,\tau}^2} \tag{13}$$

Using this relation, eqn (11) and (9) are rewritten as

$$q_{j,\tau}^{\mathrm{RC}} = \frac{1}{M_{j,\tau}} q_{j,\tau}^{\mathrm{FR}} \exp(-\beta I_{j,\tau} \bar{\omega}_{j,\tau}^2/M_{j,\tau}^2) I_0(\beta I_{j,\tau} \bar{\omega}_{j,\tau}^2/M_{j,\tau}^2) \tag{14}$$

and

$$f_{j,\tau} = \frac{\bar{\omega}_{j,\tau}\sqrt{2\pi\beta I_{j,\tau}}}{M_{j,\tau}} \exp(-\beta I_{j,\tau} \bar{\omega}_{j,\tau}^2/M_{j,\tau}^2) I_0(\beta I_{j,\tau} \bar{\omega}_{j,\tau}^2/M_{j,\tau}^2) \tag{15a}$$

Notice that eqn (15a) can be rearranged to

$$f_{j,\tau} = \frac{\sqrt{2\pi\beta k_{j,\tau}}}{M_{j,\tau}} \exp(-\beta k_{j,\tau}/M_{j,\tau}^2) I_0(\beta k_{j,\tau}/M_{j,\tau}^2) \tag{15b}$$

which shows that $f_{j,\tau}$ is independent of $I_{j,\tau}$. This situation results because both the numerator and denominator of eqn (9) have the same functional dependence on $I_{j,\tau}$. The inclusion of the Z_j factor (discussed next) restores the expected dependence of the partition function on the moments of inertia as the high-T limit is approached. Note also that the modified Bessel function $I_0(x)$ approaches $\frac{\exp(x)}{\sqrt{2\pi x}}$ as x approaches infinity; therefore, when the temperature approaches zero, *i.e.*, β approaches infinity, all the $f_{j,\tau}$ become 1, and the MS-AS partition function reduces to the MS-HO partition function. Consequently, the MS-AS and MS-HO methods yield the same zero-point energy (ZPE).

Next we consider two corrections, both introduced *via* the factor Z_j, which ensure that we reach a correct high-temperature limit. One is to replace the normal-mode partition function in the high-T limit by an internal-coordinate (local-mode)[59,60] one, and the other is to correct for kinetic energy coupling of the torsions to one another. The factor Z_j is written for this purpose as

$$Z_j = \frac{g_j Q_{\mathrm{rot},j} Q_j^{\mathrm{HO}} + (1-g_j) Q_j^{\mathrm{imp}}}{Q_{\mathrm{rot},j} Q_j^{\mathrm{HO}}} \tag{16}$$

where Q_j^{imp} is an improved approximation, $g_j \to 1$ at low T where the effects of rotational-vibrational coupling are minimal, and $g_j \to 0$ at high T. We will approximate Q_j^{imp} as

$$Q_j^{\mathrm{imp}} = Q_{\mathrm{rot},j} Q_j^{\mathrm{HO}} Z_j^{\mathrm{int}} Z_j^{\mathrm{coup}} \tag{17}$$

where the Z_j^{int} replace the normal-mode vibrational partition functions in the high-T limit by internal-coordinate ones, and Z_j^{coup} replaces the uncoupled moments of inertia for individual torsions by values that account for their coupling.

Before considering the approximations used for g_j, Z_j^{int}, and Z_j^{coup} we need to consider the high-T limit of the denominator of eqn (16):

$$\lim_{T\to\infty} Q_{\mathrm{rot},j} Q_j^{\mathrm{HO}} = \frac{\sqrt{\pi}}{\sigma_{\mathrm{rot},j}} \left(\frac{2}{\hbar^2\beta}\right)^{3/2} \left|\det \mathbf{I}_j^{\mathrm{rot}}\right|^{1/2} \left(\frac{1}{\hbar\beta}\right)^{F} \prod_{m=1}^{F} \omega_{j,m}^{-1} \tag{18}$$

where $\mathbf{I}_j^{\mathrm{rot}}$ is the 3×3 moment of inertia matrix for overall rotation of structure j and $\omega_{m,j}$ is a normal-mode frequency. We do not factor the vibrational part of eqn (18) into a stretch-bend factor and a torsion factor because we avoid assigning torsions to specific normal modes.

At high-temperature the torsions become more separable from the other vibrations and it is reasonable to replace the product of normal-mode frequencies in eqn (18) by the product of the $\bar{\omega}_{j,\tau}$ torsional frequencies and $F - t$ stretch-bend frequencies $\bar{\bar{\omega}}_{j,\bar{\bar{m}}}$ in the space orthogonal to the torsions. Note that $\bar{\bar{m}}$ is a generalized mode label that is not based on normal modes. In particular we take

$$Z_j^{\mathrm{int}} = \frac{\prod_{\bar{\bar{m}}=1}^{F-t} \bar{\bar{\omega}}_{j,\bar{\bar{m}}}^{-1} \prod_{\tau=1}^{t} \bar{\omega}_{j,\tau}^{-1}}{\prod_{m=1}^{F} \omega_{j,m}^{-1}} \tag{19}$$

where the $\bar{\bar{\omega}}_{j,\bar{\bar{m}}}$ are obtained from the Wilson GF matrix method[53–58]

$$\mathbf{GFL} = \mathbf{L\Lambda} \tag{20}$$

where the dimensions of the **G** and **F** matrices are reduced to $(F - t) \times (F - t)$, **L** is the matrix of the generalized normal mode eigenvectors, **Λ** is the eigenvalue matrix and its diagonal elements are the square of the vibrational frequencies. The **F** matrix in internal coordinates is obtained by

$$\mathbf{F} = \mathbf{A}^{\mathrm{T}} \mathbf{F}^{\mathrm{Cart}} \mathbf{A} \tag{21}$$

where **A** is the generalized inverse of the Wilson **B** matrix, $\mathbf{F}^{\mathrm{Cart}}$ is the force constant matrix in Cartesian coordinates, and T denotes a transpose. The Wilson **B** matrix constructed here only contains the non-torsional internal coordinates and the rows for torsional internal coordinates are removed; therefore its dimension is $(F - t) \times 3N$. The G matrix is given by

$$\mathbf{G} = \mathbf{BuB}^{\mathrm{T}} \tag{22}$$

where **u** is a diagonal matrix with the reciprocals of the atomic masses on the diagonal. We note that whereas the $f_{j,\tau}$ do not depend on the moments of inertia, as shown in eqn (15b), the product $Q_j^{\mathrm{HO}} Z_j^{\mathrm{int}} \prod_{\tau=1}^{t} f_{j,\tau}$ approaches the uncoupled-torsion high-T limit given by $\prod_{\bar{m}=1}^{F-t} \left(\hbar\beta\bar{\omega}_{j,\bar{m}}\right)^{-1} \prod_{\tau=1}^{t} q_{j,\tau}^{\mathrm{FR}}/P_{j,\tau}$.

Next, we consider Z_j^{coup}. In eqn (5) and (12)–(15), we employ the torsional moment-of-inertia approximation of Pitzer,[46] which is the best one can do for a torsion uncoupled to other torsions; however, we can obtain a more accurate result by allowing the torsions to be coupled to one another. To account for this coupling in the free-rotor high-T limit we need a correction factor equal to

$$Z_j^{\mathrm{coup}} = \left(\frac{|\det \mathbf{D}_j|}{\prod_{\tau=1}^{t} I_{j,\tau}} \right)^{1/2} \tag{23}$$

where **D** is the kinetic energy matrix for internal rotation of Kilpatrick and Pitzer.[47]

Finally we consider g_j. A simple expression having the correct limits and the approximately correct functional form[7] is

$$g_j = \left(\prod_{\tau=1}^{t} \tanh \frac{q_{j,\tau}^{\mathrm{FR}}}{P_{j,\tau} q_{j,\tau}^{\mathrm{CHO}}} \right)^{1/t} \tag{24a}$$

and eqn (24a) can be rearranged to

$$g_j = \left(\prod_{\tau=1}^{t} \tanh \frac{\sqrt{2\pi k_{j,\tau}\beta}}{M_{j,\tau}} \right)^{1/t} \tag{24b}$$

From a computational point of view we note that the partition function is independent of $|\det \mathbf{D}_j|$ and $\bar{\omega}_{j,\tau}$ when $g_j \to 1$.

Eqn (4), (15b), (16) and (24b) constitute our final result for the MS-AS method. Therefore, the MS-AS method does not require any saddle point optimization or scanning to determine torsional barriers, and one only needs information for each minimum.

The thermodynamic functions for the free energy, average energy, and entropy using the MS-AS method are given in Appendix B. Alternative variants of the MS-AS method are given in Appendix C.

II.B.2 Alternative derivation. In section II.B.1 the MS-AS method was introduced *via* an ansatz in which we assumed that the spacing between structures along a particular torsional coordinate τ was approximately uniform. We now present a derivation of the MS-AS approximation from an alternative point of view.

If we assume that the torsional motion is uncoupled to the remaining degrees of freedom, the partition function would factor as

$$Q \approx Q_{\perp} Q^{\mathrm{torsions}} \tag{25}$$

where $Q_{\perp}$ denotes the contribution to the total partition function from all non-torsional degrees of freedom. The quantum mechanical torsional partition function could be approximated by a classical mechanical (CM) configuration integral scaled by a Pitzer–Gwinn quantum mechanical (QM) correction factor, F^{PG},

$$Q^{\mathrm{torsions}} \approx F^{\mathrm{PG}} Q^{\mathrm{torsions,CM}} \tag{26}$$

and the classical mechanical torsional partition function could be approximated as[47]

$$Q^{\mathrm{torsions,CM}} = \left(\frac{1}{2\pi\beta\hbar^2}\right)^{t/2} (\det\{\mathbf{D}\})^{1/2} \int_0^{2\pi/\sigma_1} \cdots \int_0^{2\pi/\sigma_t} d\phi_1 \cdots d\phi_t \exp[-\beta V(\phi_1, \ldots, \phi_t)] \tag{27}$$

where the torsional kinetic energy matrix, **D**, is evaluated at the global minimum and its coordinate dependence has been neglected. We now assume that the topography of the torsional subspace is characterized by J distinct basins each characterized by a (local-)minimum-energy structure. We further assume that we can subdivide the torsional space into a set of disjoint subdomains Ω_j. If we relax the requirement of eqn (25) so that the torsional motion is only uncoupled from the remaining degrees of freedom within a particular subdomain we obtain the approximation

$$Q = \sum_{j=1}^{J} Q_{j\perp} \left(\frac{1}{2\pi\beta\hbar^2}\right)^{t/2} (\det\{\mathbf{D}_j\})^{1/2} F_j^{\mathrm{PG}} \int_{\Omega_j} d\phi_1 \cdots d\phi_t \exp[-\beta V(\phi_1, \ldots, \phi_t)] \tag{28}$$

We proceed by approximating the subdomains Ω_j as

$$\frac{-\pi}{\bar{M}_{j,\tau}} \le \phi_\tau - \bar{\phi}_{j,\tau} \le \frac{\pi}{\bar{M}_{j,\tau}};\ \tau = 1, \ldots, t \tag{29}$$

where $\bar{M}_{j,\tau}$ can be integer or non-integer, and $\bar{\phi}_{j,\tau}$ denotes the center of the subdomain j. The requirement that the subdomains span the entire torsional subspace leads to the result that

$$\sum_{j=1}^{J} \prod_{\tau=1}^{t} \frac{\sigma_\tau}{\bar{M}_{\tau,j}} = 1 \tag{30}$$

We further assume that the potential is separable in the torsional coordinates within a subdomain, *i.e.*, that

$$V(\phi_1, \ldots, \phi_t) \approx \sum_{\tau=1}^{t} V_{j,\tau}(\phi_\tau) \tag{31}$$

and that the separable 1-D potentials may be approximated as

$$V_{j,\tau} = U_j + \frac{W_{j,\tau}}{2}[1 - \cos \tilde{M}_{j,\tau}(\phi_\tau - \phi_{\tau,\mathrm{eq},j})] \tag{32}$$

where the $\phi_{\tau,\mathrm{eq},j}$ denote, as before, the equilibrium torsion angles of structure j, the $\tilde{M}$ are periodicity parameters, and the remaining parameters are the same as discussed in section II B.1. We define

$$\bar{P}_j = \frac{\bar{M}_j}{\sigma_\tau} \tag{33}$$

and

$$\tilde{P}_{j,\tau} = \frac{\tilde{M}_{j,\tau}}{\sigma_\tau} \tag{34}$$

The expression in eqn (28) reduces to the MS-AS approximation if we take

$$Q_{j\perp} = Q_{\mathrm{rot},j} \exp(-\beta U_j) Q_j^{\mathrm{HO}} \frac{Z_j}{Z_j^{\mathrm{coup}}} \prod_{\tau=1}^{t} \frac{1}{q^{\mathrm{QHO}}(\bar{\omega}_{j,\tau})} \tag{35}$$

where $q^{\mathrm{QHO}}(\bar{\omega}_{j,\tau})$ is a quantum mechanical harmonic oscillator partition function for an oscillator with a frequency $\bar{\omega}_{j,\tau}$ given by eqn (5), the Pitzer–Gwinn correction factors are calculated *via*

$$F_j^{\mathrm{PG}} = \prod_{\tau=1}^{t} \frac{q^{\mathrm{QHO}}(\bar{\omega}_{j,\tau})}{q^{\mathrm{CHO}}(\bar{\omega}_{j,\tau})} \tag{36}$$

and if we take

$$\bar{M}_{j,\tau} = \tilde{M}_{j,\tau} = M_{j,\tau}, \tag{37}$$

From the above derivation we can see that the parameter $M_{j,\tau}$ plays three roles in the MS-AS method. Firstly, it controls the local periodicity by means of eqn (8) and (32). Secondly, it determines the implicit barrier height by eqn (13). Thirdly, it determines the volume of the torsional subspace spanned by a particular structure.

II.C MS-ASCB method

In this section we present a higher-level MS method that explicitly includes the conformational barrier (CB) heights and barrier positions in the $f_{j,\tau}$ by using the segmented reference Pitzer–Gwinn[14,61] (SRPG) approximation; this is called the MS-ASCB method, where ASCB denotes "based on all structures and conformational barriers". In the SRPG approximation, a more realistic reference potential is obtained by interpolating the region between each barrier and well with its own reference potential. This yields a continuous torsional potential given by

$$V_{j,\tau} = \begin{cases} U_j + \frac{W_{j,\tau}^{L}}{2}\left[1 - \cos\left(\frac{(\phi_\tau - \phi_{\tau,\mathrm{eq},j})\pi}{(\phi_{\tau,\mathrm{eq},j} - \phi_{j,\tau}^{\mathrm{L}})}\right)\right]; & \phi_{j,\tau}^{\mathrm{L}} \le \phi_\tau \le \phi_{\tau,\mathrm{eq},j} \\ U_j + \frac{W_{j,\tau}^{R}}{2}\left[1 - \cos\left(\frac{(\phi_\tau - \phi_{\tau,\mathrm{eq},j})\pi}{(\phi_{j,\tau}^{\mathrm{R}} - \phi_{\tau,\mathrm{eq},j})}\right)\right]; & \phi_{\tau,\mathrm{eq},j} \le \phi_\tau \le \phi_{j,\tau}^{\mathrm{R}} \end{cases} \tag{38}$$

This scheme yields

$$f_{j,\tau}^{\text{MS-ASCB}} = \sigma_\tau \left[\frac{q_{j,\tau}^{\mathrm{SRC}}}{q_{j,\tau}^{\mathrm{CHO}}}\right] \tag{39}$$

where

$$q_{j,\tau}^{\mathrm{SRC}} = q_{j,\tau}^{\mathrm{FR}} \left[\frac{(\phi_{\tau,\mathrm{eq},j} - \phi_{j,\tau}^{\mathrm{L}})}{2\pi} \exp(-\beta W_{j,\tau}^{\mathrm{L}}/2) I_0(\beta W_{j,\tau}^{\mathrm{L}}/2) + \frac{(\phi_{j,\tau}^{\mathrm{R}} - \phi_{\tau,\mathrm{eq},j})}{2\pi} \exp(-\beta W_{j,\tau}^{\mathrm{R}}/2) I_0(\beta W_{j,\tau}^{\mathrm{R}}/2)\right] \tag{40}$$

the zero of energy is taken as U_j, $W_{j,\tau}^{\mathrm{L}}$ and $W_{j,\tau}^{\mathrm{R}}$ are the left and right barrier heights, respectively, for torsion mode τ of structure j, and $\phi_{j,\tau}^{\mathrm{L}}$ and $\phi_{j,\tau}^{\mathrm{R}}$ are the locations of these barriers. In contrast to the MS-AS scheme, the barrier heights in the SRPG method have to be calculated by scans or by optimizing all saddle points connecting all the structures, which adds significant computational cost and human effort.

II.D MS-AS method for strongly coupled torsions

Occasionally a subset of the torsional coordinates may be so strongly coupled that it is difficult or impossible to assign a set of $M_{j,\tau}$ parameters in the MS-AS method, even when allowing for non-integer values as suggested in II.B.2. For such cases we present a strongly coupled option for the MS-AS method that is parameterized by Voronoi tessellation.[42–44]

In the strongly coupled MS-AS scheme we partition the torsional space into a set of nearly separable (NS) coordinates and a set of strongly coupled (SC) coordinates. In general, the strongly coupled coordinates may be further partitioned into two or more subspaces, with each subspace involving only those coordinates that are strongly coupled to each other. However, for simplicity in the following discussion, we will outline only the case for a single subspace of SC coordinates; the generalization to treat multiple subspaces of SC coordinates is straightforward. We will denote the number of NS coordinates as t_{NS} and the number of SC coordinates as t_{SC}, where $t_{\mathrm{NS}} + t_{\mathrm{SC}} = t$, and we will label particular coordinates in these subspaces by subscripts τ_{NS} and τ_{SC}, respectively.

Voronoi tessellation divides a space into cells around a discrete set of points. In our application, the space to be tessellated is described by the dihedral angles $\phi_1,\phi_2,\ldots,\phi_{t_{\mathrm{SC}}}$ and the points correspond to structures. Each cell corresponds to a specific structure and consists of all torsional configurations closer to this structure than to any other structure when only the t_{SC} strongly coupled degrees of freedom are considered. We used the Euclidean norm for our distance metric. In principle, we could work with only the symmetry unique portion of the torsional space; however, because we choose to work with ordinary dihedral angles rather than symmetrized coordinates, and (as discussed earlier) these coordinates can display slight deviations from the true symmetry of the system, we do not exploit symmetry in this portion of the calculation. Thus, in order to tessellate the space we include two kinds of points. The first kind is the coordinates (sets of t_{SC} dihedral angles) of the distinguishable structures; the second kind is the coordinates of minima of the potential energy function that correspond to indistinguishable structures but where the angles are determined by adding $2\pi/\sigma_{\tau_{\mathrm{SC}}}$ to selected angles of the associated distinguishable structure. We label the points $\tilde{j} = 1, 2,\ldots, \tilde{J}$, where $\tilde{J}$ is greater than or equal to J. For example, if we were treat the torsions of propane as strongly coupled (actually they are nearly separable), we would have $J = 1$ and $\tilde{J} = 9$. We label the points as $\tilde{j} = 1, 2,\ldots, J$ for distinguishable structures and $\tilde{j} = J + 1, J + 2,\ldots, \tilde{J}$ for indistinguishable structures. One may then calculate the volume $\Omega_{\tilde{j}}^{\mathrm{SC}}$ of each cell and associate that volume with that point. We calculate the cell volumes using the convex hull code *hull* of Clarkson.[62,63] In order to properly handle the periodic nature of the coordinates, we include periodic replicas in the tessellation calculation.

By definition, the volume of the SC torsional subspace neglecting indistinguishability of identical particles is

$$\Omega^{\mathrm{SC,tot}} = \sum_{j=1}^{\bar{J}} \Omega_j^{\mathrm{SC}} = (2\pi)^{t_{\mathrm{SC}}} \tag{41}$$

After accounting for indistinguishability, the total volume of the SC torsional subspace may be calculated by

$$\Omega^{\mathrm{SC}} = \sum_{j=1}^{J} \Omega_j^{\mathrm{SC}} \tag{42}$$

we should find that

$$\frac{\Omega^{\mathrm{SC}}}{\Omega^{\mathrm{SC,tot}}} = \frac{1}{\sigma_1\sigma_2\ldots\sigma_{t_{\mathrm{SC}}}} \tag{43}$$

but slight deviations may occur due to symmetry distortions resulting from the limitations of working in a coordinate system of ordinary dihedral angles. In such cases it may be desirable to rescale the distinguishable volumes so that this equality holds exactly or to work with volumes that are averages of selected structures that are related by additional symmetries (see the later discussion of mirror image structures of pentyl radical for an example).

When the torsional subspace is so strongly coupled that we cannot assign $M_{j,\tau_{\mathrm{SC}}}$ by considerations based on considering each torsion separately, then we replace all $M_{j,\tau_{\mathrm{SC}}}$ for strongly coupled torsions of a given j by a single M_j^{SC} equal to

$$M_j^{\mathrm{SC}} = \frac{2\pi}{(\Omega_j^{\mathrm{SC}})^{1/t_{\mathrm{SC}}}} \tag{44}$$

When this is done, eqn (30) with $\bar{M}_{j,\tau}$ replaced by $M_{j,\tau}$ is automatically satisfied if eqn (43) holds.

When the SC method is used, the intrinsically separable effective potentials of eqn (8) are no longer defined. The strongly coupled MS-AS scheme is not a classical partition function, augmented by a Pitzer–Gwinn quantum correction, for a particular effective torsional potential. Instead, it is an interpolation scheme that yields correct values in the low- and high-temperature limits and gives reasonable values between these limits.

If one treats all the coordinates as if they constitute a single set of strongly coupled coordinates, then the Voronoi tessellation, together with the equations above, provides a fully automatable way of assigning the M parameters. However, grouping nearly separable degrees of freedom together with strongly coupled ones results in an approximation in which the contribution to the partition function of the nearly separable torsions is not expected to be as accurate as when one uses the method of section II.B.1 for these torsions. Thus, we recommend keeping the dimensions of the SC subspaces as small as is feasible. That is, we recommend assigning torsions to SC subspaces only when they are coupled so strongly that we cannot assign $M_{j,\tau_{\mathrm{SC}}}$ values based on considering each torsion separately.

II.E MS-RS method

Although wherever feasible we strongly recommend the inclusion of all structures in the partition function calculation, as is done in the MS-AS scheme, we recognize that a lower level of treatment is needed in some circumstances where the harmonic approximation is qualitatively incorrect and where finding and optimizing all structures requires too much work. In such instances, we propose a reference-structure treatment involving the generation of structures by independent torsions. To apply this method, one chooses one structure as a reference structure, and one considers only the other structures that can be generated by independently rotating the torsions, one at a time. One can start from any reasonable reference structure. If any structure among the generated structures is found to have a lower energy than the starting structure, one can optionally start over taking this lower-energy structure as the new reference structure. The number of structures that needs to be optimized for this approach scales linearly with the number of torsions, t, so for large molecules it can be much more affordable than the MS-AS scheme where the number of structures scales exponentially with t.

Label the reference structure as $j = 1$, and number the distinguishable structures, which are denoted $j[\tau, i(\tau)]$, generated by rotating about torsional coordinate τ in the reference structure as $i(\tau) = 1,\ldots, P_{1,\tau}$ We adopt the convention that $i(\tau) = 1$ corresponds to a null rotation, which leads to the reference structure for every τ. We define the multi-structure reference-structure (MS-RS) approximation to the conformational-rovibrational partition function as

$$Q_{\mathrm{con\text{-}rovib}}^{\mathrm{MS\text{-}RS}} = Q^{\mathrm{ref}} \prod_{\tau=1}^{t} \sum_{i(\tau)=1}^{P_{1,\tau}} \frac{Q_{j[\tau,i(\tau)]}^{\mathrm{IT}}}{Q_{j=1}^{\mathrm{IT}}} \tag{45}$$

where

$$Q^{\mathrm{ref}} = Q_{\mathrm{rot},1} \exp(-\beta U_1) Q_1^{\mathrm{HO}} Z_1 \prod_{\tau'=1}^{t} f_{1,\tau'} \tag{46}$$

$$Q_j^{\mathrm{IT}} = Q_{\mathrm{rot},j} \exp(-\beta U_j) Q_j^{\mathrm{HO}} Z_j \prod_{\tau'=1}^{t} P_{j,\tau'} f_{j,\tau'} \tag{47}$$

and the remaining quantities are the same as those discussed for the MS-AS method. Notice that in eqn (46) we set $j = 1$, which denotes the reference structure. If the reference structure is not the lowest-energy structure included, then U_1 need not be zero (as it was in the MS-AS and MS-ASCB methods); in general, U_j is 0 for the lowest-energy structure included in eqn (45), and for all the other structures, U_j is the equilibrium potential energy relative to the lowest-energy structure included. The inclusion of the $P_{j,}$ factor in eqn (47) results in the Q_j^{IT} being scaled by a quantity proportional to the volume of the torsional subspace spanned by this structure; thus, the ratio of factors in eqn (45) properly accounts for the differences in the domain sizes of the various structures. Notice $P_{j,\tau}$ used in MS-RS method is obtained from $M_{j,\tau}$ and σ_τ by eqn (1).

Notice that the $P_{j,\tau}$ and σ_τ are not directly needed for the MS-AS method (unlike $M_{j,\tau}$, they cancel out in the final equations, although their knowledge is useful for ascertaining whether or not all the structures are accounted for); however, the MS-RS method explicitly requires the $P_{j,\tau}$ (or the σ_τ from which they may be calculated by eqn (1)) as well as $M_{j,\tau}$.

Except for the $P_{j,\tau}$, the MS-RS method requires no information that is not needed for MS-AS calculations, and it requires information for only a subset of the structures. In cases where a subset of torsional motions are strongly coupled the MS-RS scheme may not perform as well as when the coupling is small; in such instances one may seek extensions of the MS-RS scheme that, for instance, treat the NS torsions independently but which include additional structures obtained by modifying the reference structure by two or more simultaneous rotations from within the SC torsional subspace. Such extensions may provide additional accuracy while retaining the desirable computational scaling of the MS-RS approach, but they are beyond the scope of the present study.

III. Calculations and results

To illustrate the MS methods, we apply the MS-HO, MS-AS, and MS-ASCB methods to two one-dimensional (1-D) model potentials and to ethanol. Note that the MS-AS and MS-RS methods are identical for some simple cases such as ethanol and 1-D potentials. However, we will compare the MS-HO, MS-AS, and MS-RS methods for 1-butanol and 1-pentyl radical in the present study.

The M06-2X[64] density functional was used for calculating the geometries and energetics of ethanol and the 1-pentyl radical, and the MPW1K[65] density functional was used for 1-butanol. The 6-311 + G(2df,2p) basis set[66,67] was used for all the calculations. All density functional calculations were performed using the *Gaussian 09* program.[68]

Because *meta*-GGA density functionals are sensitive to integration grids, we performed a grid-convergence analysis on the frequencies of ethanol and 1-pentyl radical using the M06-2X/6-311 + G(2df,2p) method. As shown in Table 1, the frequencies calculated by M06-2X/6-311 + G(2df,2p) are well converged when one uses the density functional integration grid that has 99 radial shells around each atom and 974 angular points in each shell. Therefore this grid (99,974) was used for all M06-2X calculations in this article. The pruned (99,590) grid, which is called *ultrafine* in *Gaussian09*, was used for calculations with the MPW1K functional, which are less sensitive to the fineness of the integration grids.

Table 1 Normal-mode frequencies (cm^{-1}) calculated by M06-2X/6-311 + G(2df,2p) accompanied various integration grids

Grids	Ethanol (structure: E–t), 3 lowest frequencies				
Ultrafine[a]	224	269	423		
(99,590)[b]	224	268	423		
(99,770)[b]	247	292	423		
(99,974)[b]	238	278	422		
(96,32,64)[c]	236	275	423		
	1-Pentyl radical (structure: P–stt), 5 lowest frequencies				
Ultrafine[a]	53*i*	84	126	225	287
(99,590)[b]	75	85	127	225	287
(99,770)[b]	64	85	128	228	287
(99,974)[b]	76	87	129	228	287
(120,974)[b]	75	87	129	228	287
(150,974)[b]	75	87	129	229	287
(96,32,64)[c]	71	87	128	228	287

[a] Ultrafine denotes the pruned (99,590) grid provided in the *Gaussian09* package. [b] The first number indicates the number of radial quadrature nodes, and the second denotes the number of Lebedev angular quadrature nodes. [c] A spherical product grid with the first number specifying the number of radial quadrature nodes and the next two specifying the numbers of angular quadrature nodes.

Table 2 Notation for torsion angles[a]

	Abbreviation	Dihedral angle range (deg)
Antiperiplanar	a^+	[140, 163]
	a^-	[−163, −140]
Gauche for 1-pentyl	g^+	[55, 80]
	g^-	[−80, −55]
Or		
Gauche for 1-butanol	g^+	[57, 76]
	g^-	[−76, −57]
Cross for 1-butanol only	x^+	[80, 90]
	x^-	[−90, −80]
Syn for 1-pentyl only	s	[80, 100] or [−100, −80]
Trans	t	[−173, −180] and [180, 173]

[a] The dihedral angles used for torsions are H–O–$C^{(1)}$–$C^{(2)}$, O–$C^{(1)}$–$C^{(2)}$–$C^{(3)}$, and $C^{(1)}$–$C^{(2)}$–$C^{(3)}$–$C^{(4)}$ for 1-butanol, H–$C^{(1)}$–$C^{(2)}$–$C^{(3)}$, $C^{(1)}$–$C^{(2)}$–$C^{(3)}$–$C^{(4)}$, and $C^{(2)}$–$C^{(3)}$–$C^{(4)}$–$C^{(5)}$ for 1-pentyl, and H–O–C–C and O–C–C–H for ethanol.

All the minima of ethanol, 1-pentyl radical, and 1-butanol are fully optimized and confirmed by normal-mode analysis. The saddle points of ethanol that connect the minima are also optimized and are confirmed to have one imaginary frequency.

Table 2 shows the notation that is used for torsion angles in this paper. This notation is based on standard notation but is also specialized to the needs of the present study.

Partition functions are calculated from 100 K to 50 000 K. The 50 000 K result is tabulated not because this is an accessible temperature, but rather to illustrate the high-temperature limit for formal purposes.

The frequencies ($\omega_{j,m}$, $\bar{\omega}_{j,\tau}$, and $\bar{\bar{\omega}}_{j,\bar{\bar{m}}}$) used in the calculations (except in the 1–D cases) are all scaled, and the scaling factors designed to give accurate ZPEs are used.[69]

We also employed Benson's group additivity (GA) method[30,31,70] to calculate entropies of ethanol, 1-pentyl radical, and 1-butanol for comparison. For this purpose we use not only Benson's[30] group parameters but also those of Cohen[31] and Lay *et al.*[34]

III.A 1-D models

In order to better understand the proposed methods, we first apply them to two 1-D torsion models. One is an artificial 1-D model potential designed to show the effect of a shallow minimum, and the other is the 1-D torsion potential of H_2O_2 from the work of Koput *et al.*[71] that has been used in a prior study[14] of torsional methods.

The first 1-D model potential is given by

$$V/\mathrm{cm}^{-1} = 121.352549 + 90.0\cos(2\phi) + 60.0\cos(3\phi) \quad (48)$$

where ϕ is the torsion angle. This potential has three minima in the range of $[0, 2\pi)$ and we assume they are all distinguishable, *i.e.*, $M = P = 3$. This potential is plotted in Fig. 1, and the rotational barrier heights and the locations of minima are also given in the figure. The internal moment of inertia is assumed to be 1.53618 amu Å^2 and to be independent of ϕ.

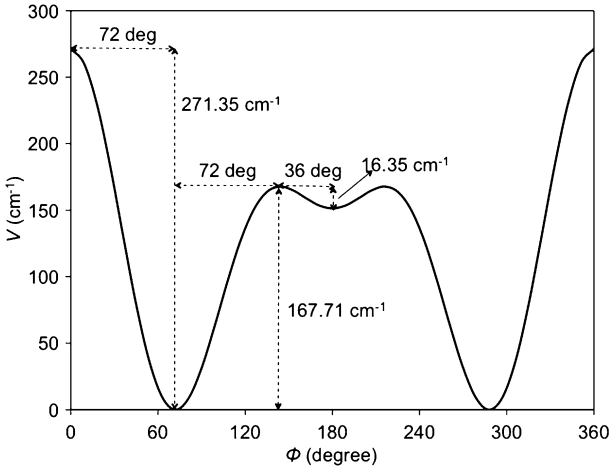

Fig. 1 A model potential (eqn (48)) representing a torsional motion.

The harmonic frequencies calculated using eqn (5) are 126.41 and 62.85 cm^{-1} for the deep and shallow minima, respectively.

The small barriers and the presence of a very shallow minimum for this potential make it an interesting model to test the proposed methods. The accurate partition functions were calculated by the torsional eigenvalue summation (TES) method.[14] The calculated partition functions and the percentage errors of the approximate schemes relative to the TES values are listed in Table 3.

Table 4 shows the errors of the multi-structural methods when the shallow minimum is ignored (because the MS-ASCB method requires information for all the barriers, it is not included in Table 4.). When ignoring this shallow well, we set $M = P = 2$ which alters the effective barrier heights of the reference potential.

The 1-D torsional potential for H_2O_2 is given by[71]

$$V/\mathrm{cm}^{-1} = 811.3053546 + 1037.4\cos(\phi) + 674.2\cos(2\phi) + 46.9\cos(3\phi) + 2.7\cos(4\phi) \quad (49)$$

This potential energy curve is plotted together with the heights and locations of the barriers in Fig. 2. The minima

Table 3 Calculated partition functions and their percentage errors compared to TES values for the 1-D model potential of eqn (48)

	MS-HO		MS-AS		MS-ASCB		TES
T/K	q	% error	q	% error	q	% error	q
60	0.4776	−17	0.5247	−9	0.5356	−7	0.5751
100	1.083	−14	1.236	−2	1.229	−3	1.266
150	1.935	−10	2.174	1	2.132	−1	2.159
200	2.863	−5	3.078	2	3.006	−1	3.025
300	4.848	5	4.703	2	4.596	−0	4.600
400	6.922	16	6.106	2	5.983	0	5.979
600	11.18	35	8.447	2	8.315	0	8.303
1000	19.87	67	12.06	1	11.93	0	11.92
1500	30.83	100	15.55	1	15.44	0	15.42
2000	41.82	128	18.43	1	18.33	0	18.31
2400	50.62	149	20.46	1	20.36	0	20.34
3000	63.83	177	23.17	0	23.08	0	23.07
4000	85.87	218	27.11	0	27.03	0	27.02
7000	152.0	318	36.48	0	36.42	0	36.41
50 000	1100	1007	99.43	0	99.40	0	99.40

Table 4 Percentage errors of various methods compared to TES values for the torsion potential of eqn (48) when the shallow minimum on the model potential is ignored

T/K	MS-HO	MS-AS
60	−20	−17
100	−24	−19
150	−28	−20
200	−30	−20
300	−29	−17
400	−27	−15
600	−21	−11
1000	−8	−7
1500	7	−5
2000	20	−4
2400	30	−3
3000	43	−3
4000	63	−2
7000	111	−1
50 000	453	−0

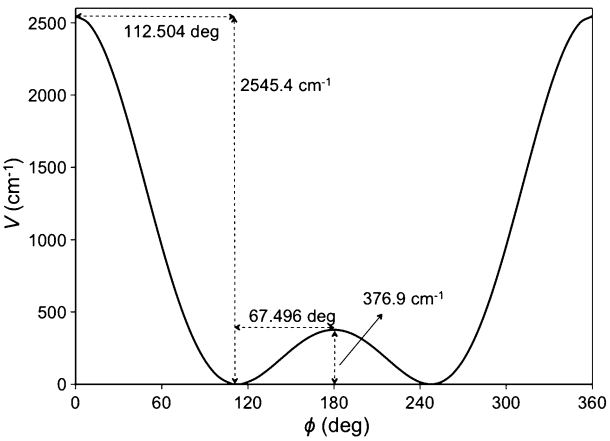

Fig. 2 The potential energy curve (eqn (49)) of the 1-D torsional motion in H_2O_2.

are mirror-image structures and are therefore distinguishable ($J = P = M = 2$). The internal moment of inertia is 0.423202 amu Å^2 and the harmonic frequency of each minimum is 382.6 cm^{-1}. This 1-D potential has been studied in a previous paper[14] in which the effective barrier height used in the RPG scheme was chosen as the average of the two barrier heights. In the MS-AS method (which also uses the RPG scheme for torsions), the effective barrier height is calculated by eqn (13).

Table 5 lists the calculated partition functions and the percentage errors of the approximate schemes relative to the TES values for the 1-D potential of H_2O_2.

III.B Ethanol

The ethanol molecule has two torsions. One involves internal rotation about the C–C bond, and the other involves internal rotation about the C–O bond. If the torsions are considered separately, they each have 3 minima along their torsion coordinates. The torsion around the C–C bond only has one distinguishable minimum because the three hydrogen atoms of the methyl group are identical whereas the torsion around the C–O bond leads to 3 distinguishable minima. Although two of these structures are isoenergetic, they are mirror images and

Table 5 Calculated partition functions and their percentage errors compared to TES values for the 1-D model potential of H_2O_2

	MS-HO		MS-AS		MS-ASCB		TES
T/K	q	% error	q	% error	q	% error	q
60	0.02036	−34	0.02061	−33	0.01999	−35	0.03071
100	0.1281	−23	0.1308	−21	0.1281	−23	0.1654
150	0.3276	−18	0.3386	−15.	0.3364	−16	0.3990
200	0.5395	−16	0.5656	−12	0.5655	−12	0.6442
300	0.9509	−15	1.03	−8	1.018	−9	1.116
400	1.345	−14	1.501	−3	1.443	−7	1.555
600	2.105	−11	2.443	4	2.223	−6	2.359
1000	3.588	−5	4.199	11	3.616	−5	3.787
1500	5.419	1	6.089	13	5.187	−4	5.383
2000	7.244	6	7.707	13	6.621	−3	6.827
2400	8.701	10	8.856	12	7.684	−3	7.893
3000	10.88	16	10.4	11	9.158	−2	9.366
4000	14.52	26	12.63	9	11.35	−2	11.56
7000	25.43	51	17.86	6	16.65	−1	16.83
50 000	181.7	255	51.67	1	51.08	−0	51.17

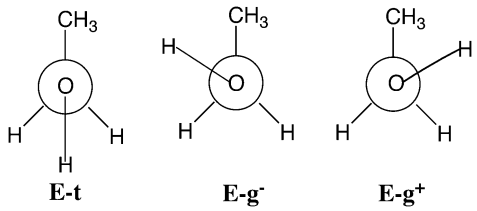

Fig. 3 Newman projections of the three structures of ethanol. Structure E–t is the global minimum and structures E–g$^-$ and E–g$^+$ are isoenergetic but distinguishable. Note that E denotes ethanol, t denotes *trans*, and g denotes *gauche*.

thus distinguishable. Therefore, as shown in Fig. 3, the ethanol molecule, with two torsions, has three distinguishable structures that contribute to the total partition function.

Table 6 lists the information used in the MS-AS and MS-ASCB calculations for ethanol. Table 7 lists the partition function calculated using the MS-HO, MS-AS, and MS-ASCB methods.

Fig. 4 shows the percentage difference of the partition functions of structure E–t from that of E–g$^+$ or E–g$^-$ using the harmonic approximation. Note that each harmonic partition function used here takes its own minimum as the zero of energy.

Fig. 5 shows the ratio of the partition function of ethanol calculated by the multi-structural method to that calculated by

Table 6 Information used for the ethanol partition function calculations using the MS-AS and MS-ASCB methods[a]

Torsion	$\bar{\omega}$	W^b	W^L	W^R	I	M	P
Structure E–t (U_1 = 0)							
C–O	258.7	328.9	385.7	385.7	0.7456	3	3
C–C	253.9	1108.6	1108.7	1108.7	2.610	3	1
Structure E–g$^+$ & E–g$^-$ (U_2 = U_3 = 27.4 cm^{-1})							
C–O	278.5	379.0	358.6	372.0	0.7416	3	3
C–C	264.5	1206.2	1194.9	1194.9	2.616	3	1

[a] The units are cm^{-1} for the barrier heights and frequencies and amu Å^2 for the internal moments of inertia. [b] W is used in the MS-AS method and is calculated by eqn (13).

Table 7 Calculated conformational-rovibrational partition function of ethanol using multi-structural methods

T/K	MS-HO	MS-AS	MS-ASCB
100	4.12E−104	4.47E−104	4.37E−104
150	5.45E−68	6.21E−68	6.08E−68
200	8.13E−50	9.64E−50	9.46E−50
300	1.95E−31	2.43E−31	2.39E−31
400	4.77E−22	6.06E−22	6.00E−22
600	2.94E−12	3.73E−12	3.70E−12
1000	1.62E−03	1.90E−03	1.89E−03
1500	3.60E + 02	3.65E + 02	3.65E + 02
2000	7.76E + 05	6.84E + 05	6.83E + 05
2400	7.65E + 07	6.06E + 07	6.06E + 07
3000	1.74E + 10	1.19E + 10	1.19E + 10
4000	1.56E + 13	8.67E + 12	8.67E + 12
7000	6.07E + 18	2.15E + 18	2.15E + 18
50 000	1.13E + 38	6.34E + 36	6.34E + 36

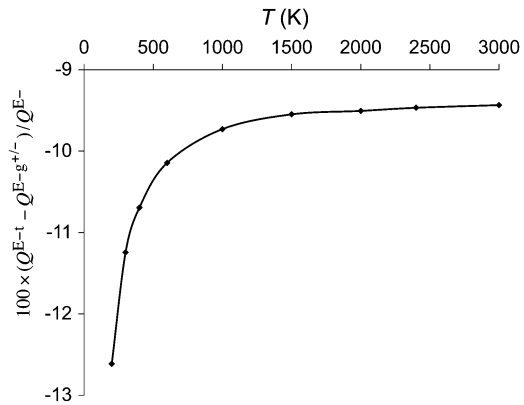

Fig. 4 Percentage difference between partition functions of structures E–t and E–g$^-$ (or E–g$^+$) using the harmonic approximation. The zero of energy is at each structure's local minimum.

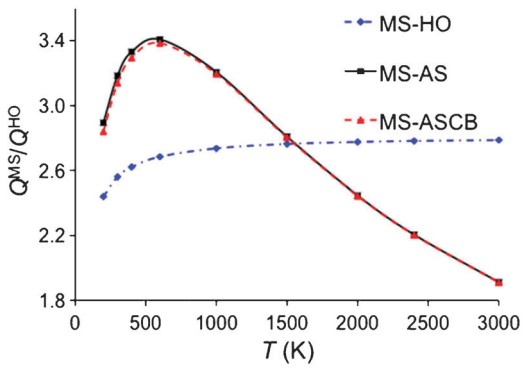

Fig. 5 Ratio of the rovibrational partition function of ethanol calculated by multi-structural methods to that calculated by the single-structure HO approximation at the global minimum.

the single-structure HO (SS-HO) approximation (J, Z_j, and $f_{j,\tau}$ are equal to 1) at the global minimum (E–t).

III.C 1-pentyl radical

The 1-pentyl radical has four torsions that are associated with internal rotation about each of the four C–C bonds. We label the five carbon atoms as: $H_2C^{(1)}$–$H_2C^{(2)}$–$H_2C^{(3)}$–$H_2C^{(4)}$–$H_3C^{(5)}$, and the four torsions are around the 1–2, 2–3, 3–4, and 4–5 C–C bonds, respectively. The 1-pentyl

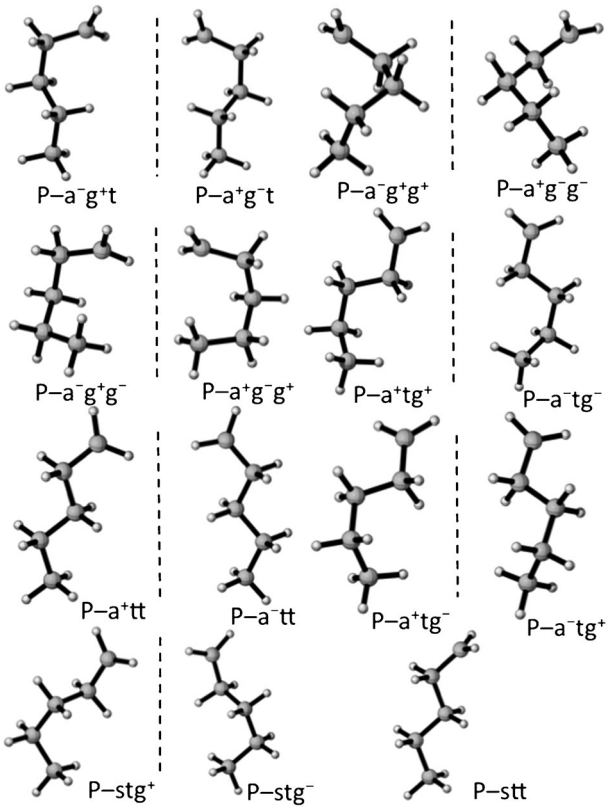

Fig. 6 Fifteen structures of the 1-pentyl radical. Structures separated by a dashed vertical line are mirror images, *e.g.*, P–a$^-$g$^+$t and P–a$^+$g$^-$t.

radical constitutes an example of a system displaying significant torsional coupling, in particular involving the $\tau = 1$ ($C^{(1)}$–$C^{(2)}$) and $\tau = 2$ ($C^{(2)}$–$C^{(3)}$) internal rotations; assigning $M_{j,\tau}$ parameters in such circumstances merits special care. In the absence of steric hindrance effects,[37–39] torsion involving a –CH_2 radical group is expected to have 6-fold periodicity and low barrier heights yielding three distinguishable minima. The 4–5 torsion is expected to have three total minima, only one of which is a distinguishable minimum, and the other two torsions are expected to have three total minima, all distinguishable. Thus, an uncoupled model would lead one to expect a total of 27 distinguishable structures. However, the total number of distinguishable structures of 1-pentyl radical is found to be only 15 as shown in Fig. 6. The 15 structures include seven pairs of mirror-image structures (which of course have the same energy and vibrational frequencies); therefore we only need to perform electronic structure calculations on eight of the 15 structures. In larger systems steric effects can lead to either a larger or smaller number of structures than would be expected based on a separable approximation.[40,51]

In the absence of strong coupling the structures should correspond closely to minima encountered when the system is rotated about a single torsional coordinate. In this limit, $P_{j,\tau}$ assignments (and thus $M_{j,\tau}$ assignments after taking account of the torsional symmetry) may be made by starting with a particular structure, choosing a τ, and counting all structures (including the starting structure) that have similar torsional angles to the starting structure for every torsion except the τ torsion. This approach confirms the expected results of $P_{j,\tau=3} = 3$ and $P_{j,\tau=4} = 1$ for all values of j. A similar exercise for the $\tau = 1$ torsion leads to 9 structures with expected values of $P_{j,\tau=1} = 3$ and six structures (P–a$^-$g$^+$t, P–a$^+$g$^-$t, P–a$^-$g$^+$g$^+$, P–a$^+$g$^-$g$^-$, P–a$^-$g$^+$g$^-$, P–a$^+$g$^-$g$^+$) with $P_{j,\tau=1} = 1$.

Relaxed scans starting from each of these six latter structures reveal a single broad structure spanning the entire 180 degrees of the symmetry-unique $\tau = 1$ torsional degree of freedom each with a relatively large barrier—the effective barriers estimated by eqn (13) range from 451 to 654 cm^{-1} (using $M = 2$) as compared to values of 29 to 44 cm^{-1} (using $M = 6$) for the other 9 structures. The occurrence of these broad minima may be considered to arise from steric hindrance effects that outweigh the small barriers that one would anticipate existing between 3 expected structures in the absence of such steric effects. Thus, each of the 3 structures with broad features along the $\tau = 1$ coordinate may be thought of as aggregations of 3 expected structures and therefore these structures span a torsional subspace with a volume that is approximately 3 times as large as that spanned by the remaining 9 structures having assignments of $P_{j,\tau=1} = 3$.

In the absence of steric effects we would anticipate assignments of $P_{j,\tau=2} = 3$ for each of the structures, and such assignments would be consistent with the sum of the torsional subspace volumes of each of the structures totalling to the total volume (see eqn (30)), which serves as a convenient consistency check of possible assignments. Rigid scans along the $\tau = 2$ torsional coordinate reveal 3 distinct minima, but due to strong coupling with the $\tau = 1$ torsional degree of freedom, not all of these minima correspond closely with other structures. In particular, if we select a particular structure and look for all other structures having similar torsional angles for all torsional coordinates other than $\tau = 2$, we find either 0 or 1 additional structures and this suggests that the simple scheme for assigning $P_{j,\tau}$ values breaks down in the presence of strong torsional coupling. For example, if we start by considering the P–a$^-$g$^+$t structure we find only the P–a$^-$tt structure corresponds closely to the starting structure *via* a rotation about the $\tau = 2$ coordinate. In the presence of strong torsional coupling we need to generalize our criteria for assigning $P_{j,\tau}$ so that instead of looking only for structures having similar torsional angles to that of the structure undergoing assignment along $t - 1$ coordinates we look for structures for which the spans of the torsional minima strongly overlap with each of the spans of the torsional minima of the starting structure along $t - 1$ coordinates. Under this relaxed set of criteria we see that the P–a$^+$g$^-$t structure, which is one of the structures having a single broad minima along $\tau = 1$, overlaps with the torsional spans of P–a$^-$g$^+$t along the required $t - 1$ coordinates even though the $\tau = 1$ torsional angles of these two structures differ by about 54 degrees. Under this relaxed set of search criteria we are easily able to identify two other structures that are sufficiently similar to each structure undergoing assignment to yield assignments of $P_{j,\tau=2} = 3$ for all structures.

When employing the MS-RS method we need to identify all structures obtained by independent rotations from a reference structure. In this context, if we consider the reference structure to be P–a$^-$g$^+$t, the structures most consistent with independent

rotation about the $\tau = 2$ coordinate are the P–a$^-$tt and P–a$^+$g$^-$t structures. One of these is the mirror image structure of the reference structure, which shows that the concept of an independent internal rotation about a single torsional coordinate must be considered as highly approximate in the presence of strong torsional coupling. As we will see in the following, the results for the MS-RS and MS-AS methods show good consistency suggesting that both methods can, at least sometimes, yield reasonable partition functions even for cases where we have strong torsional coupling.

We also consider two variants of the strongly coupled option of the MS-AS scheme, one (denoted NS : SC = 2 : 2) which treats the 1–2 and 2–3 torsions as strongly coupled and one (denoted NS : SC = 1 : 3) which treats the 1–2, 2–3, and 3–4 torsions as strongly coupled. These methods not only take account of the strong coupling, but they eliminate the need for much of the analysis presented in the proceeding four paragraphs.

In the NS : SC = 2 : 2 scheme, the 15 structures are divided into 3 groups with the structures in each group having the same torsional conformation for the 3–4 torsion. In particular, the group with the 3–4 torsion in a *trans* conformation includes the structures P–a$^-$g$^+$t, P–a$^+$g$^-$t, P–a$^+$tt, P–a$^-$tt, and P–stt; the group with the 3–4 torsion in a g$^+$ conformation includes the structures P–a$^-$g$^+$g$^+$, P–a$^+$g$^-$g$^+$, P–a$^+$tg$^+$, P–a$^-$tg$^+$, and P–stg$^+$; and the group for with the 3–4 torsion in a g$^-$ conformation includes the structures P–a$^+$g$^-$g$^-$, P–a$^-$g$^+$g$^-$, P–a$^-$tg$^-$, P–a$^+$tg$^-$, and P–stg$^-$. The Voronoi tessellation is performed considering each group separately.

In the Voronoi tessellation calculations, some indistinguishable structures are generated by symmetry. For example, if the P–a$^+$tt struture is denoted by its first three torsional angles as (159.7, 178.8, 179.9) its corresponding indistinguishable structure is (−20.3, 178.8, 179.9) due to the 2-fold symmetry of the –CH_2 radical group. The angles 159.7 degrees and −20.3 degrees refer to the dihedral angle H_a–$C^{(1)}$–$C^{(2)}$–$C^{(3)}$ and H_b–$C^{(1)}$–$C^{(2)}$–$C^{(3)}$. However, the optimized structure has the H_b–$C^{(1)}$–$C^{(2)}$–$C^{(3)}$ angle as −30.4 degrees. This discrepancy is caused by using a dihedral angle to represent the torsion,

Table 8 Information used for the 1-pentyl radical partition function using the multi-structural method[a]

			NS : SC = 2 : 2			NS : SC = 1 : 3			NS : SC = 4 : 0		
Torsion	$\bar{\omega}$	I	W^b	M	P	W^b	M	P	W^b	M	P
Structure P–a$^-$g$^+$t & P–a$^+$g$^-$t (U = 0)											
$C^{(1)}$–$C^{(2)}$	133	1.714	281	2.53	1.27	254	2.67	1.33	451	2	1
$C^{(2)}$–$C^{(3)}$	142	10.91	2047	2.53	2.53	1846	2.67	2.67	1458	3	3
$C^{(3)}$–$C^{(4)}$	99	15.98	1040	3	3	1316	2.67	2.67	1040	3	3
$C^{(4)}$–$C^{(5)}$	228	2.917	998	3	1	998	3	1	998	3	1
Structure P–a$^-$g$^+$g$^+$ & P–a$^+$g$^-$g$^-$ (U = 27.0 cm^{-1})											
$C^{(1)}$–$C^{(2)}$	161	1.713	426	2.48	1.24	380	2.63	1.31	654	2	1
$C^{(2)}$–$C^{(3)}$	131	17.09	2819	2.48	2.48	2512	2.63	2.63	1924	3	3
$C^{(3)}$–$C^{(4)}$	108	18.38	1418	3	3	1852	2.63	2.63	1418	3	3
$C^{(4)}$–$C^{(5)}$	247	3.054	1228	3	1	1228	3	1	1228	3	1
Structure P-a$^-$g$^+$g$^-$ & P–a$^+$g$^-$g$^+$ (U = 349.4 cm^{-1})											
$C^{(1)}$–$C^{(2)}$	157	1.713	382	2.56	1.28	336	2.73	1.36	625	2	1
$C^{(2)}$–$C^{(3)}$	132	15.88	2521	2.56	2.56	2216	2.73	2.73	1831	3	3
$C^{(3)}$–$C^{(4)}$	110	14.79	1188	3	3	1437	2.73	2.73	1188	3	3
$C^{(4)}$–$C^{(5)}$	254	3.057	1297	3	1	1297	3	1	1297	3	1
Structure P–a$^+$tg$^+$ & P–a$^-$tg$^-$ (U = 229.8 cm^{-1})											
$C^{(1)}$–$C^{(2)}$	126	1.670	81	4.40	2.20	107	3.84	1.92	44	6	3
$C^{(2)}$–$C^{(3)}$	110	14.45	533	4.40	4.40	698	3.84	3.84	1146	3	3
$C^{(3)}$–$C^{(4)}$	125	11.48	1177	3	3	717	3.84	3.84	1177	3	3
$C^{(4)}$–$C^{(5)}$	229	3.039	1049	3	1	1048	3	1	1049	3	1
Structure P–a$^+$tt & P–a$^-$tt (U = 73.8 cm^{-1})											
$C^{(1)}$–$C^{(2)}$	118	1.661	76	4.28	2.14	94	3.82	1.91	38	6	3
$C^{(2)}$–$C^{(3)}$	119	11.40	523	4.28	4.28	655	3.82	3.82	1063	3	3
$C^{(3)}$–$C^{(4)}$	117	11.91	1079	3	3	664	3.82	3.82	1079	3	3
$C^{(4)}$–$C^{(5)}$	227	2.871	976	3	1	976	3	1	976	3	1
Structure P–a$^+$tg$^-$ & P–a$^-$tg$^+$ (U = 257.4 cm^{-1})											
$C^{(1)}$–$C^{(2)}$	109	1.668	64	4.30	2.15	81	3.82	1.91	33	6	3
$C^{(2)}$–$C^{(3)}$	107	14.518	536	4.30	4.30	679	3.82	3.82	1098	3	3
$C^{(3)}$–$C^{(4)}$	123	11.34	1135	3	3	701	3.82	3.82	1135	3	3
$C^{(4)}$–$C^{(5)}$	228	3.040	1041	3	1	1041	3	1	1041	3	1
Structure P–stg$^+$ & P–stg$^-$ (U = 294.9 cm^{-1})											
$C^{(1)}$–$C^{(2)}$	103	1.670	82	3.57	1.79	92	3.36	1.68	29	6	3
$C^{(2)}$–$C^{(3)}$	109	15.34	845	3.57	3.57	954	3.36	3.36	1196	3	3
$C^{(3)}$–$C^{(4)}$	124	11.53	1161	3	3	925	3.36	3.36	1161	3	3
$C^{(4)}$–$C^{(5)}$	229	3.039	1051	3	1	1051	3	1	1051	3	1
Structure P–stt (U = 124.6 cm^{-1})											
$C^{(1)}$–$C^{(2)}$	108	1.650	90	3.56	1.78	100	3.39	1.69	32	6	3
$C^{(2)}$–$C^{(3)}$	121	11.88	816	3.56	3.56	901	3.39	3.39	1150	3	3
$C^{(3)}$–$C^{(4)}$	116	11.96	1068	3	3	837	3.39	3.39	1068	3	3
$C^{(4)}$–$C^{(5)}$	232	2.878	1024	3	1	1024	3	1	1024	3	1

[a] The units are cm^{-1} for barrier heights and frequencies and amu Å^2 for internal moments of inertia. [b] W is used in the MS-AS method and is calculated by eqn (13).

Table 9 Calculated conformational-rovibrational partition function of 1-pentyl radical using multi-structural methods

		MS-AS			
T/K	MS-HO	2 : 2[a]	1 : 3[a]	4 : 0[a]	MS-RS
100	5.11E−190	6.02E−190	6.10E−190	5.53E−190	6.32E−190
150	1.83E−124	2.22E−124	2.27E−124	1.93E−124	2.09E−124
200	2.04E−91	2.50E−91	2.59E−91	2.11E−91	2.16E−91
300	6.69E−58	8.22E−58	8.61E−58	6.72E−58	6.45E−58
400	1.05E−40	1.28E−40	1.35E−40	1.04E−40	9.66E−41
600	1.14E−22	1.34E−22	1.42E−22	1.12E−22	1.01E−22
1000	2.20E−06	2.21E−06	2.31E−06	1.97E−06	1.78E−06
1500	2.74E+04	2.13E+04	2.20E+04	1.99E+04	1.82E+04
2000	6.18E+10	3.71E+10	3.81E+10	3.56E+10	3.29E+10
2400	4.06E+14	2.01E+14	2.05E+14	1.95E+14	1.82E+14
3000	1.37E+19	5.17E+18	5.27E+18	5.07E+18	4.78E+18
4000	6.57E+24	1.69E+24	1.71E+24	1.67E+24	1.59E+24
7000	4.08E+35	4.37E+34	4.40E+34	4.35E+34	4.22E+34
50 000	7.38E+72	1.98E+70	1.98E+70	1.97E+70	1.96E+70

[a] NS : SC.

which also has the effect that some mirror images have slightly different volumes (*e.g.* the volumes of P–a$^+$tt and P–a$^+$tt have about a 1% difference). If the two mirror images have different volumes, we used the averaged volume to calculate M values.

The structure P–a$^-$g$^+$t (the global minimum) is chosen as the reference structure in the MS-RS calculations. Independent rotations starting from this reference structure generate the structures P–a$^-$g$^+$g$^+$, P–a$^-$g$^+$g$^-$, P–a$^-$tt, and P–a$^+$g$^-$t. These five structures are used in the MS-RS calculations.

Table 8 lists information for each structure of 1-pentyl radical that is used for the partition function calculations using various schemes for M values. Table 9 lists the partition functions of 1-pentyl radical calculated by the MS-HO, MS-AS, and MS-RS methods.

Fig. 7 shows the percentage differences of the harmonic oscillator partition functions of three structures relative to that of structure P–a$^-$g$^+$t or P–a$^+$g$^-$t (each harmonic oscillator partition function takes its own minimum as the zero of energy). Fig. 8 shows the ratios of the partition function of 1-pentyl radical calculated by multi-structural methods to those calculated by the SS-HO approximation at the global minimum (P–a$^-$g$^+$t or P–a$^+$g$^-$t).

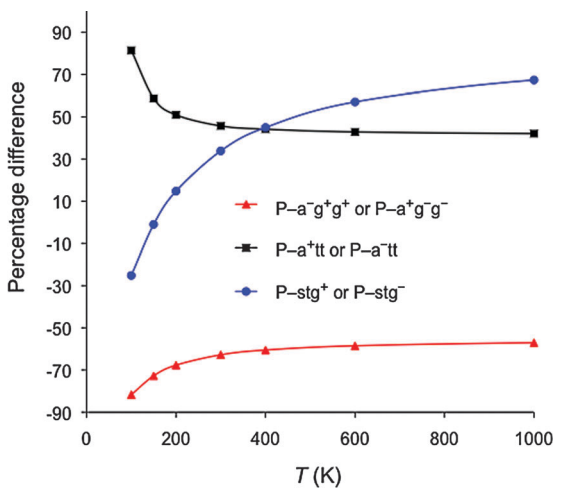

Fig. 7 Percentage difference between harmonic oscillator partition functions of the global minimum structure and selected other structures of the 1-pentyl radical. The zero of energy is at each structure's local minimum. The three cases with the largest difference are presented in this figure.

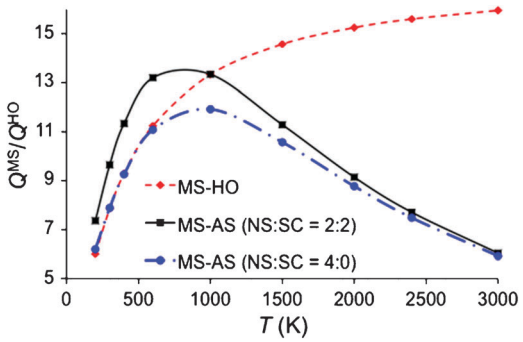

Fig. 8 Ratio of the partition function of the 1-pentyl radical calculated by multi-structural methods to that calculated by the single-structure HO approximation using the global minimum structure.

III.D 1-Butanol

We label the carbon atoms in 1-butanol as HO–$H_2C^{(1)}$–$H_2C^{(2)}$–$H_2C^{(3)}$–$H_3C^{(4)}$. The four torsions in 1-butanol are associated with internal rotation around each of the three C–C bonds and one C–O bond. Each torsion, with the exception of the methyl torsion, is expected to generate 3 distinguishable structures, and a total of 27 distinguishable structures is expected to be generated. However, due to steric hindrance between the terminal hydroxyl and methyl groups, the expected structures g$^+$g$^-$g$^+$ and g$^-$g$^+$g$^-$ are saddle points that connects g$^+$x$^-$g$^+$/g$^+$g$^-$x$^+$ and g$^-$x$^+$g$^-$/g$^-$g$^+$x$^-$ structures, respectively. A similar effect has also been observed in alkanes.[17,51] Therefore, 1-butanol has a total of 29 structures. The 29 structures include 14 pairs of mirror-image structures; therefore, electronic structure calculations only needed to be performed for 15 structures. Two previous conformational studies[72,73] of 1-butanol only observed 27 structures with the structures assigned as g$^+$g$^-$g$^+$ and g$^-$g$^+$g$^-$ being similar to our g$^+$x$^-$g$^+$ and g$^-$x$^+$g$^-$ structures. The g$^+$x$^-$g$^+$ structure has torsional angles (for torsions 1–2, 2–3, and 3–4, respectively) of 60.0, 82.3, and 59.8, the g$^-$g$^+$x$^-$ structure has torsional angles of 73.4, −63.3, and 88.2, and the intervening transition state has torsional angles of 73.2, –68.9, and 81.9 degrees. The g$^+$x$^-$g$^+$ and g$^-$g$^+$x$^-$ structures lie 149 and 8 cm^{-1} below the intervening transition state, respectively.

The structure B–tg$^+$t is chosen as the reference structure in the MS-RS calculations. Starting from this reference structure, one can generate the structures B–g$^+$g$^+$t, B–g$^-$g$^+$t, B–ttt, B–tg$^-$t, B–tg$^+$g$^-$, and B–tg$^+$g$^+$ by independent rotation of each C–C bond or C–O bond. These seven structures are used in the MS-RS calculations.

If there were no steric hindrance effect in 1-butanol such that the torsions only generated 27 structures, the parameter $M_{j,\tau}$ would be 3 for each torsion. However, it is not trivial to set reasonable integer values of $M_{j,\tau}$ for the 29 structures that satisfy eqn (30). Therefore, we use the MS-AS method with NS : SC = 1 : 3 to determine the $M_{j,\tau}$ values by treating only the methyl group torsion as NS.

Given that the $g^+x^-g^+/g^+g^-x^+$ ($g^-x^+g^-/g^-g^+x^-$) structures overlap very strongly and the $g^+g^-x^+$ ($g^-g^+x^-$) structure is extremely shallow (being bound by only 7.9 cm^{-1}) it is reasonable to only include the lower energy structure of each pair in an MS-AS calculation involving 27 structures.

Table 10 lists the information for each structure of 1-butanol that is needed for the partition function calculations. Table 11 gives the calculated conformational-rovibrational partition functions of 1-butanol.

Table 12 lists the standard state entropy of ethanol, 1-pentyl radical, and 1-butanol calculated from SS-HO, MS-HO, and MS-AS partition functions including contributions from electronic and translational degrees of freedom, and also calculated using Benson's group additivity method; the global minimum structure is used for the SS-HO method. Table 12 also contains experimentally derived values[74,75] for comparison.

Table 13 lists the calculated correction factors Z^{int} and Z^{coup} for structures of ethanol, 1-butanol, and 1-pentyl radical.

Fig. 9 shows the two cases with the largest percentage difference of structure-specific harmonic oscillator partition functions relative to that of the global minimum (each harmonic oscillator partition function takes its own minimum as the zero of energy). Fig. 10 plots the temperature dependence of the ratio of the partition function of 1-butanol calculated by the multi-structural methods to that calculated by the SS-HO approximation at the global minimum.

IV. Discussion

We will begin by comparing the new MS-AS methods to accurate results of 1-D models so that we can demonstrate their accuracy for treating intra-mode anharmonicity without complications from mode-mode coupling and anharmonicities of other vibrational modes. We have already extensively studied[14] methods to treat the intra-mode anharmonicity; herein we will only compare to the accurate values from torsional eigenvalue summation. Expansion of a torsional potential in terms of a Fourier series, along with the assumption of a constant moment of inertia, leads to a banded symmetric matrix that may be diagonalized with negligible computational expense. This technique has a long history[14,19,20,76–81] and it might seem tempting to apply it whenever the additional energy evaluations needed for fitting the Fourier potential are affordable. However, there is little benefit to treating the intramode anharmonicity to a much higher degree of accuracy than we can treat the intermode anharmonicity; this is especially true in applications[19,20] where multiple torsional modes are so treated because coupling between torsional degrees of freedom is often very important. Treatment of the inter-mode anharmonicity, which we achieve primarily by including multiple structures, is a much harder task and the primary goal of the new methods presented herein, but we begin by demonstrating that the methods also treat intramode anharmonicity well.

Table 3 clearly shows that the MS-HO approximation significantly overestimates the torsional partition function at high temperature and modestly underestimates the torsional partition function at low temperatures for the 1-D model of eqn (48). For this model torsion and most typical torsional potentials where the barriers are not very low, the MS-HO approximation is adequate for practical work at low temperatures. Due to cancellation of error, the MS-HO approximation may have quite small errors at some temperatures (*e.g.*, 300 K for this 1-D model potential).

The MS-AS and MS-ASCB methods both use the Pitzer–Gwinn approximation based on a reference classical partition function, but they require different information about the torsional potential. They both need the energies, frequencies, and geometries of all structures that are local minima of the potential energy surface, and the MS-ASCB method also needs the locations and magnitudes of the torsional barriers. For this 1-D potential, the barriers of the deep wells are 271 cm^{-1} and 1678 cm^{-1} for each side, respectively; the shallow well has a symmetric barrier of 16 cm^{-1}. Eqn (13) gives effective barriers of 1612 cm^{-1} and 40 cm^{-1} for the deep and shallow wells, respectively. Although the MS-AS and MS-ASCB methods use different effective barriers, they both have errors of less than 3% for the potential of eqn (48) at temperatures above 100 K. The predominant source of errors of both methods at low temperatures (*e.g.*, 60 K) is the Pitzer–Gwinn approximation, which only puts the quantum effects in at a harmonic level.

For the 1-D model potential of eqn (48), there is a very shallow minimum as shown in Fig. 1. On the potential energy surface of a real molecule, the geometry of such a shallow minimum may be hard to find and optimize. Also for complex molecules, finding all possible shallow minima may prove difficult, so we consider the consequences of neglecting them for this model problem. When the shallow minimum is ignored, the calculated effective barrier using eqn (13) is 364 cm^{-1} with $M = P = 2$. Table 4 shows that for $T < 1000$ K the two multi-structural methods (MS-HO and MS-AS) both underestimate the partition function when using two minima compared to that calculated by using three minima. At higher temperatures the MS-AS method has errors smaller than 7% when the shallow minimum is ignored. In the high-temperature limit (illustrated by 50 000 K), the error of the MS-AS method is negligible even without explicitly accounting for the shallow minimum because the torsional partition function approaches a free rotor partition function, which is independent of the potential. These results suggest that accounting for shallow minima can be important if their energies are low (151.36 cm^{-1} in the 1-D model potential of eqn (48)) especially at temperatures of 400 K and lower.

The exact barrier heights on the two sides of each minimum for the 1-D torsional potential of H_2O_2 (eqn (49)) are 2545 cm^{-1} and 377 cm^{-1}, and this large difference presents a significant challenge for the MS-AS method as it assumes a single barrier height. The effective mean barrier height calculated by eqn (13) and used in the MS-AS method is 919 cm^{-1}. Although this value is quite different from the exact ones, Table 5 shows that the MS-AS method has errors no larger than 13% from 200 to 3000 K, with the largest error at 1500 K, where the error corresponds to an error of only 0.36 kcal mol^{-1} in the free energy. This 1-D case shows that accurate barrier height information does improve the accuracy of the calculated partition function through the use of the MS-ASCB method, but that the calculated partition function is not too sensitive to the barrier heights. Because one of the two barriers on this potential energy surface is very high, the MS-HO approximation gives adequate results from 300 to 2400 K.

Table 10 Information used for the 1-butanol conformational-rovibrational partition function using multi-structural methods[a]

Torsion	$\bar{\omega}$	I	NS : SC = 1 : 3			27-structures, NS : SC = 4 : 0		
			W^b	M	P	W^b	M	P
Structure B–ttt (U = 16.6 cm^{-1})								
$O^{(1)}$–$C^{(1)}$	244	0.763	281	3.10	3.10	300	3	3
$C^{(1)}$–$C^{(2)}$	122	10.800	989	3.10	3.10	1057	3	3
$C^{(2)}$–$C^{(3)}$	112	11.391	881	3.10	3.10	942	3	3
$C^{(4)}$–$C^{(5)}$	231	2.832	995	3	1	995	3	1
Structure B–ttg$^+$ & B–ttg$^-$ (U = 329.5 cm^{-1})								
$O^{(1)}$–$C^{(1)}$	250	0.755	307	3.02	3.02	310	3	3
$C^{(1)}$–$C^{(2)}$	107	13.624	1012	3.02	3.02	1023	3	3
$C^{(2)}$–$C^{(3)}$	119	10.829	1000	3.02	3.02	1010	3	3
$C^{(4)}$–$C^{(5)}$	218	3.001	944	3	1	944	3	1
Structure B–tg$^+$t & B–tg$^-$t (U = 0.0 cm^{-1})								
$O^{(1)}$–$C^{(1)}$	243	0.759	273	3.12	3.12	296	3	3
$C^{(1)}$–$C^{(2)}$	143	10.368	1284	3.12	3.12	1391	3	3
$C^{(2)}$–$C^{(3)}$	98	15.608	914	3.12	3.12	990	3	3
$C^{(4)}$–$C^{(5)}$	229	2.879	994	3	1	994	3	3
Structure B–tg$^+$g$^+$ & B–tg$^-$g$^-$ (U = 229.9 cm^{-1})								
$O^{(1)}$–$C^{(1)}$	247	0.766	320	2.94	2.94	308	3	3
$C^{(1)}$–$C^{(2)}$	114	16.178	1433	2.94	2.94	1378	3	3
$C^{(2)}$–$C^{(3)}$	91	17.732	1008	2.94	2.94	970	3	3
$C^{(4)}$–$C^{(5)}$	220	3.007	960	3	1	960	3	1
Structure B–tg$^+$g$^-$ & B–tg$^-$g$^+$ (U = 605.4 cm^{-1})								
$O^{(1)}$–$C^{(1)}$	259	0.757	326	3.04	3.04	335	3	3
$C^{(1)}$–$C^{(2)}$	124	13.514	1345	3.04	3.04	1379	3	3
$C^{(2)}$–$C^{(3)}$	105	15.789	1116	3.04	3.04	1145	3	3
$C^{(4)}$–$C^{(5)}$	223	3.030	989	3	1	989	3	1
Structure B–g$^+$tt & B–g$^-$tt (U = 16.1 cm^{-1})								
$O^{(1)}$–$C^{(1)}$	261	0.757	320	3.09	3.09	340	3	3
$C^{(1)}$–$C^{(2)}$	128	10.938	1105	3.09	3.09	1176	3	3
$C^{(2)}$–$C^{(3)}$	112	11.538	889	3.09	3.09	946	3	3
$C^{(4)}$–$C^{(5)}$	231	2.833	1000	3	1	1000	3	1
Structure B–g$^+$tg$^+$ & B–g$^-$tg$^-$ (U = 359.0 cm^{-1})								
$O^{(1)}$–$C^{(1)}$	252	0.760	301	3.08	3.08	318	3	3
$C^{(1)}$–$C^{(2)}$	110	13.915	1040	3.08	3.08	1100	3	3
$C^{(2)}$–$C^{(3)}$	118	10.981	949	3.08	3.08	1004	3	3
$C^{(4)}$–$C^{(5)}$	217	3.001	933	3	1	933	3	1
Structure B–g$^+$tg$^-$ & B–g$^-$tg$^+$ (U = 314.4 cm^{-1})								
$O^{(1)}$–$C^{(1)}$	265	0.770	356	3.00	3.00	357	3	3
$C^{(1)}$–$C^{(2)}$	112	13.886	1146	3.00	3.00	1149	3	3
$C^{(2)}$–$C^{(3)}$	119	11.012	1019	3.00	3.00	1022	3	3
$C^{(4)}$–$C^{(5)}$	217	3.003	934	3	1	934	3	1
Structure B–g$^+$g$^+$t & B–g$^-$g$^-$t (U = 40.6 cm^{-1})								
$O^{(1)}$–$C^{(1)}$	261	0.786	345	3.03	3.03	354	3	3
$C^{(1)}$–$C^{(2)}$	146	10.378	1415	3.03	3.03	1448	3	3
$C^{(2)}$–$C^{(3)}$	96	15.648	924	3.03	3.03	946	3	3
$C^{(4)}$–$C^{(5)}$	230	2.882	1000	3	1	1000	3	1
Structure B–g$^+$g$^+$g$^+$ & B–g$^-$g$^-$g$^-$ (U = 251.2 cm^{-1})								
$O^{(1)}$–$C^{(1)}$	264	0.783	382	2.91	2.91	359	3	3
$C^{(1)}$–$C^{(2)}$	114	16.244	1471	2.91	2.91	1381	3	3
$C^{(2)}$–$C^{(3)}$	89	17.861	991	2.91	2.91	930	3	3
$C^{(4)}$–$C^{(5)}$	220	3.008	961	3	1	961	3	1
Structure B–g$^+$g$^+$g$^-$ & B–g$^-$g$^-$g$^+$ (U = 598.4 cm^{-1})								
$O^{(1)}$–$C^{(1)}$	259	0.790	355	3.00	3.00	349	3	3
$C^{(1)}$–$C^{(2)}$	128	13.858	1514	3.00	3.00	1491	3	3
$C^{(2)}$–$C^{(3)}$	105	15.615	1154	3.00	3.00	1136	3	3
$C^{(4)}$–$C^{(5)}$	236	3.031	1113	3	1	1113	3	1
Structure B–g$^+$x$^-$g$^+$ & B–g$^-$x$^+$g$^-$ (U = 770.4 cm^{-1})								
$O^{(1)}$–$C^{(1)}$	260	0.770	272	3.37	3.37	343	3	3
$C^{(1)}$–$C^{(2)}$	149	15.428	1785	3.37	3.37	2253	3	3
$C^{(2)}$–$C^{(3)}$	112	13.917	904	3.37	3.37	1141	3	3
$C^{(4)}$–$C^{(5)}$	284	3.021	1603	3	1	1603	3	1
Structure B–g$^+$g$^-$t & B–g$^-$g$^+$t (U = 70.6 cm^{-1})								
$O^{(1)}$–$C^{(1)}$	254	0.767	301	3.12	3.12	326	3	3
$C^{(1)}$–$C^{(2)}$	140	10.435	1253	3.12	3.12	1355	3	3
$C^{(2)}$–$C^{(3)}$	101	15.489	966	3.12	3.12	1045	3	3
$C^{(4)}$–$C^{(5)}$	230	2.876	999	3	1	999	3	1
Structure B–g$^+$g$^-$g$^-$ & B–g$^-$g$^+$g$^+$ (U = 343.7 cm^{-1})								
$O^{(1)}$–$C^{(1)}$	237	0.766	293	2.96	2.96	285	3	3
$C^{(1)}$–$C^{(2)}$	112	16.267	1379	2.96	2.96	1342	3	3
$C^{(2)}$–$C^{(3)}$	95	17.744	1094	2.96	2.96	1065	3	3
$C^{(4)}$–$C^{(5)}$	219	3.006	947	3	1	947	3	1

Table 10 (*continued*)

Torsion	$\bar{\omega}$	I	NS : SC = 1 : 3 W^b	M	P	27-structures, NS : SC = 4 : 0 W^b	M	P
Structure B–g$^+$g$^-$x$^+$ & B–g$^-$g$^+$x$^-$ (U = 911.5 cm^{-1})								
O$^{(1)}$–C$^{(1)}$	272	0.783	271	3.55	3.55			
C$^{(1)}$–C$^{(2)}$	115	12.330	761	3.55	3.55			
C$^{(2)}$–C$^{(3)}$	117	17.289	1110	3.55	3.55			
C$^{(4)}$–C$^{(5)}$	202	3.012	810	3	1			

[a] The units are cm^{-1} for barrier heights and frequencies and amu Å^2 for internal moments of inertia. [b] W is used in the MS-AS method and is calculated by eqn (13).

Table 11 Calculated conformational-rovibrational partition function of 1-butanol using multi-structural methods

T/K	MS-HO	MS-AS NS : SC = 4 : 0[b]	MS-AS NS : SC = 1 : 3	MS-RS[a]
100	1.09E−179	1.24E−179	1.25E−179	1.10E−179
150	1.28E−117	1.57E−117	1.58E−117	1.43E−117
200	2.44E−86	3.17E−86	3.20E−86	2.95E−86
300	1.25E−54	1.79E−54	1.80E−54	1.69E−54
400	2.24E−38	3.44E−38	3.48E−38	3.31E−38
600	2.39E−21	3.91E−21	3.98E−21	3.85E−21
1000	5.18E−06	7.99E−06	8.20E−06	8.12E−06
1500	1.55E + 04	1.94E + 04	1.99E + 04	2.01E + 04
2000	1.38E + 10	1.35E + 10	1.39E + 10	1.41E + 10
2400	5.11E + 13	4.15E + 13	4.27E + 13	4.35E + 13
3000	8.66E + 17	5.39E + 17	5.53E + 17	5.65E + 17
4000	1.74E + 23	7.32E + 22	7.49E + 22	7.68E + 22
7000	2.01E + 33	3.49E + 32	3.55E + 32	3.65E + 32
50 000	1.00E + 68	4.29E + 65	4.31E + 65	4.42E + 65

[a] The reference structure is taken as B–tg$^+$t. [b] Using only 27 structures, see text for further details.

Ethanol is a simple molecule that has two torsions. As shown in Table 3, the two torsions around the C–O and C–C bonds have very close frequencies when modeled using internal coordinates. In the normal mode analysis, the two torsional motions are strongly coupled, and consequently the two lowest-frequency modes are mixtures of two torsional motions. The normal mode with the lowest frequency is the antisymmetric combination of two torsions, and the mode with the second lowest frequency is the symmetric combination. Therefore, even such a simple molecule as ethanol provides a case where it is impossible to assign the torsions to specific normal modes. The barrier heights calculated by eqn (13) are 1109, 329, 1206, and 379 cm^{-1} and agree very well with the normal modes optimized by the M06-2X/6-311 + G(2df,2p) method, which are 1109, 386, 1195, and 359 cm^{-1}.

To apply the MS-ASCB method to ethanol, one needs to calculate the torsion angle difference $\phi_{\tau,\mathrm{eq},j}-\phi^{\mathrm{L}}_{j,\tau}$ or $\phi^{\mathrm{R}}_{j,\tau}-\phi_{\tau,\mathrm{eq},j}$. For the ethanol calculations, we use a single dihedral angle to represent a torsion angle although one could also construct a torsion coordinate involving a top rotating about a fixed frame from a combination of several related dihedral angles.[48–50] The $\Delta\phi^{\mathrm{R}}$ and $\Delta\phi^{\mathrm{L}}$ of the C–C torsion are set to 60 degrees due to the symmetry. The $\Delta\phi^{\mathrm{R}}$ and $\Delta\phi^{\mathrm{L}}$ of C–O is measured by the dihedral angle H–O–C–C; they are both 61.8 and degrees for structure E–t and are both 59.1 degrees for structures E–g$^+$ and E–g$^-$.

Table 12 Standard state entropy (in cal mol^{-1} K^{-1}) calculated using SS-HO, MS-HO, and MS-AS partition functions and group additivity method[a]

T/K	SS-HO	MS-HO	MS-AS	GA	Ref. data
Ethanol					
298.15	64.79	66.85	67.47	67.10	67.31[b]
400	69.96	72.02	72.59	72.17	
600	79.26	81.33	81.68	81.16	
1000	94.99	97.06	96.85	96.28	
1-butanol					
298.15	80.04	85.97	87.17[c]	85.94	86.8[d]
400	88.54	94.78	96.07[c]	94.65	
600	104.25	110.77	111.86[c]	110.22	
1000	131.29	138.00	138.14[c]	136.48	
1-pentyl radical					
298.15	83.75	89.08	89.48[e]	86.32	
				88.48[f]	
				88.13[g]	
400	93.04	98.54	98.87[e]	95.86	
				97.87[f]	
				97.40[g]	
600	110.09	115.71	115.71[e]	112.64	
				114.55[f]	
				114.02[g]	
1000	139.20	144.88	143.95[e]	141.08	
				143.06[f]	
				142.21[g]	
1500	167.96	173.64	171.62[e]	169.22	
				171.50[f]	

[a] The SS-HO calculations only account the contribution from the global minimum and all the vibrational modes (including torsional modes) are approximated as harmonic oscillator (J, Z_j, and $f_{j,\tau}$ are all equal to 1). All the calculated entropies include electronic and translational contributions. Frequencies used in the calculations are all scaled (see text for details). The calculations by GA method use the parameters in ref. 30 except those in footnote *f* and *g*. [b] From ref. 74. [c] The data are calculated using NS : SC = 3 : 1. [d] Experimental data from ref. 75. [e] The data are calculated using NS : SC = 2 : 2. [f] The parameters used in the calculations were taken from Cohen.[33] [g] The parameters used in the GA calculations were taken from Lay *et al.*[34]

When conformational structures change by internal rotations, the other vibrational frequencies (*e.g.* stretching and bending modes) also change correspondingly. One of advantages of the multi-structural methods is that anharmonicities and couplings due to conformational changes are partially accounted for by the use of a different harmonic analysis at each structure. To illustrate the effect of conformational changes on partition functions, Fig. 4 shows the percentage difference of the ethanol E–g$^+$ or E–g$^-$ HO partition function from that of the global minimum E–t. Although the E–t and E–g$^+$ (or E–g$^-$)

Table 13 The calculated correction factors Z^{int} and Z^{coup} for structures of ethanol, 1-butanol, and 1-pentyl radical

Structure	Z^{int}	Z^{coup}	Structure	Z^{int}	Z^{coup}
Ethanol			1-butanol		
E–t	0.954	1.000	B–ttt	0.920	0.937
E–g$^+$/E–g$^-$	0.974	0.993	B–ttg$^+$/B–ttg$^-$	0.790	0.962
			B–tg$^+$t/B–tg$^-$t	0.886	0.941
1-pentyl radical			B–tg$^+$g$^+$/B–tg$^-$g$^-$	1.024	0.758
P–a$^-$g$^+$t$^-$P–a$^+$g$^-$t$^+$	0.834	0.935	B–tg$^+$g$^-$/B–tg$^-$g$^+$	0.642	0.948
P–a$^-$g$^+$g$^+$/P–a$^+$g$^-$g$^-$	1.115	0.737	B–g$^+$tt/B–g$^-$tt	0.912	0.938
P–a$^-$g$^+$g$^-$/P–a$^+$g$^-$g$^+$	0.721	0.928	B–g$^+$tg$^+$/B–g$^-$tg$^-$	0.789	0.954
P–a$^+$g$^+$g$^+$/P–a$^-$g$^-$g$^-$	0.785	0.944	B–g$^+$tg$^-$/B–g$^-$tg$^+$	0.818	0.946
P–a$^+$tt/P–a$^-$tt	0.866	0.935	B–g$^+$g$^+$t/B–g$^-$g$^-$t	0.922	0.909
P–a$^+$tg$^-$/P–a$^-$tg$^+$	0.700	0.945	B–g$^+$g$^+$g$^+$/B–g$^-$g$^-$g$^-$	1.027	0.744
P–stg$^+$/P–stg$^-$	0.608	0.938	B–g$^+$g$^+$g$^-$/B–g$^-$g$^-$g$^+$	0.770	0.908
P–stt	0.783	0.933	B–g$^+$x$^-$g$^+$/B–g$^-$x$^+$g$^-$	0.716	0.917
			B–g$^+$g$^-$t/B–g$^-$g$^+$t	0.868	0.936
			B–g$^+$g$^-$g$^-$/B–g$^-$g$^+$g$^+$	1.020	0.759
			B-g$^+$g$^-$x$^+$/B–g$^-$g$^+$x$^-$	0.554	0.934

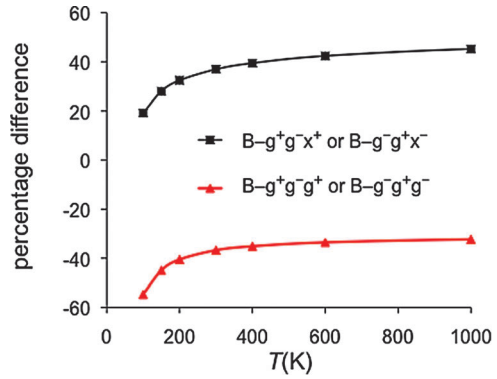

Fig. 9 Percentage difference between harmonic oscillator partition functions of selected 1-butanol structures and the harmonic oscillator partition functions of the global minimum. The zero of energy is at each structure's local minimum. The two cases with the largest differences are presented in this figure.

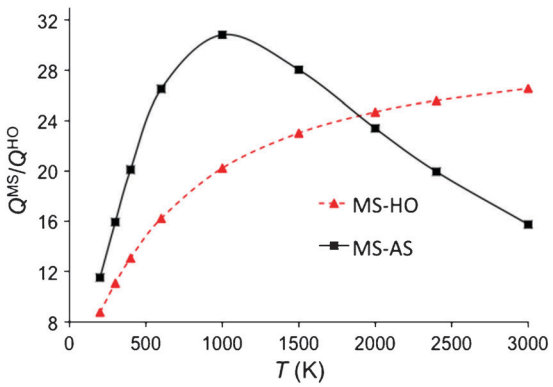

Fig. 10 Ratio of the partition function of 1-butanol calculated by multi-structural methods with NS : SC = 1 : 3 to that calculated by the single-structure HO approximation at the global minimum.

structures have quite similar conformations, this difference can be as large as 12%. The differences are larger for 1-pentyl radical and 1-butanol. Because many conformational structures of 1-pentyl radical are quite different from the global minimum, the effects of conformational changes on partition functions are very large as shown in Fig. 7. Even larger effects are observed for 1-butanol as shown in Fig. 9. Therefore, treating torsions as separable with the frequencies of the other modes fixed at their values for the global minimum structures can introduce large errors.

When the harmonic approximation is applied to calculate partition functions in the literature, often only one structure (the global minimum) is considered. Therefore we compared the ratio of partition functions calculated by multi-structural methods to those calculated by the harmonic approximation for the global minimum. Because ethanol has three conformational structures, the partition functions calculated by multi-structural methods are larger than those calculated by the HO approximation using one structure, and the factors are between 1.9 and 3.4 in the temperature range 200–3000 K as shown in Fig. 5. Because the 1-pentyl radical and 1-butanol have many more conformational structures, the partition functions calculated by the multi-structural methods are *much* larger than the harmonic ones obtained using only the global minimum structure as shown in Fig. 8 and 10, respectively. For example, at T = 1000 K, the MS-AS partition function of 1-butanol is larger than that of the SS-HO approximation by a factor of 31.

Standard state entropies calculated from the SS-HO, MS-HO, and MS-AS partition functions for ethanol, 1-pentyl radical, and 1-butanol are compared to each other and to the GA method and reference data in Table 12. The reference data for ethanol is based on spectroscopic data and a reference structure treatment of anharmonicity; the reference data for 1-butanol is based on experimental heat capacities and heats of fusion and vaporization; and there is no available reference data for the 1-pentyl radical. The entropies calculated by the MS-HO method are in much better agreement with the reference data than is the single-structure HO data, and the entropies calculated by the MS-AS method give even better agreement for both ethanol and 1-butanol at the temperature studied. The entropies calculated by various parametrizations of the GA method are also listed in Table 12 for comparison. For ethanol and 1-butanol we only calculate entropies up to 1000 K because the heat capacities C_p are available only up to 1000 K for an OH group, and extrapolation may not be reliable. All the GA calculations use the parameters from the Benson's tables[30] except some calculations for 1-pentyl radical also use the parameters from Cohen's[33] and Lay *et al.*'s[34] work. Benson has estimated[30] that "Values of C_p and

S estimated from these groups are on the average within ± 0.3 cal mol^{-1} K^{-1} of the measured values…" and "for heavily substituted species, deviations in C_p and S may go as high as ± 1.5 cal mol^{-1} K^{-1}…" We find that the difference of the GA data from the MS-AS data and the reference data sometimes exceed these estimated uncertainties. The GA calculations for 1-pentyl radical obtained using Cohen's parameters agree better with the MS-AS values than those obtained using Benson's or Lay *et al.*'s parameters.

In the intermediate-temperature region, the values of the MS-AS partition functions of ethanol, 1-pentyl (using the 2 : 2 scheme), and 1-butanol (using the 1 : 3 scheme) are larger than those of the MS-HO partition functions. However, the MS-AS partition functions of 1-pentyl radical with all four torsions treated as nearly separable are almost the same as or lower than the MS-HO partition functions. This is because the torsion around the $C^{(1)}$–$C^{(2)}$ bond in the 1-pentyl radical has a very low barrier predicted by $M = 6$, and its torsional correction factor $f_{j,\tau}$ is already smaller than 1 in the intermediate temperature region. Fig. 11 shows the temperature dependence of $f_{j,\tau}$ for several relevant cases. In the low-temperature limit the correction factors $f_{j,\tau}$ are 1, and they initially rise above 1 as temperature increases. Eventually the correction factors achieve a relative maximum and then subsequently monotonically decrease. This behavior is quite different from that predicted by the switching functions advocated in earlier work.[7]

The three sets of $M_{j,\tau}$ values (or equivalently the domain volumes) for 1-pentyl radical all have larger volumes (smaller $M_{j,\tau}$ values) for the first three pairs of structures in Table 8 than for the others, and the three sets of MS-AS partition functions have similar magnitudes. While it is difficult to judge which set of $M_{j,\tau}$ values is more accurate, this indicates that the $M_{j,\tau}$ values determined by Voronoi tessellation lead to reasonable results. The ratio of the largest to the smallest of the three sets of MS-AS partition functions at 400 K is only 1.30. It is interesting to compare the effective barrier heights calculated from the three sets of $M_{j,\tau}$ values. The radical –CH_2 group rotation barrier is around 250 cm^{-1} for the global minimum P–a^{-}g^{+}t obtained by a relaxed scan. The effective barrier heights calculated by $M = 2.67$ (254 cm^{-1}) and $M = 2.53$ (281 cm^{-1}) have better agreement with the barrier height obtained by a relaxed scan than that calculated by $M = 2$ (451 cm^{-1}). However, for the structure P–stt, the effective barrier height obtained by a relaxed scan (around 30–40 cm^{-1}) is much lower than that calculated with $M = 3.39$ (100 cm^{-1}) and $M = 3.56$ (90 cm^{-1}), but it agrees very well with the barrier height calculated with $M = 6$ (32 cm^{-1}). Despite these differences between the effective barrier heights calculated by the three different sets of $M_{j,\tau}$ values, all of the calculated effective barrier heights fall into reasonable ranges for all the torsions considered here. The three sets of MS-AS partition functions of 1-pentyl radical have the same high–T limit because the torsional partition function is independent of the $M_{j,\tau}$ values in the high–T limit as long as eqn (30) is satisfied.

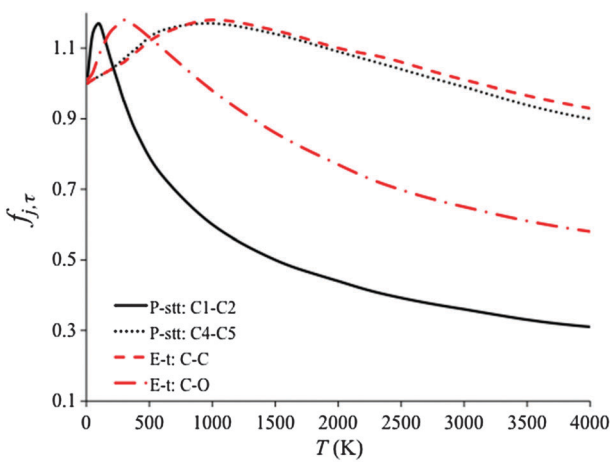

Fig. 11 Temperature dependence for the $f_{j,\tau}$ for several relevant cases.

For 1-butanol the 27-structures partition functions and 29-structures partition functions have differences of less than 3% because the two addtitional structures have high energies and small subdomain volumes. This result shows that missing some structures with high energies need not lead to large errors in applying the MS-AS method.

For 1-butanol, the MS-AS partition functions and MS-RS partition functions agree with each other within about 3% for 600 K and above, but the deviation rises to 6% and 8% at 300 K and 200 K, respectively. For the 1-pentyl radical, the deviations between the MS-AS and MS-RS partition functions are larger than those for 1-butanol but are still within 10% for temperatures above 200 K when both are calculated with integer $M_{j,\tau}$. The differences between the 1-pentyl MS-RS and MS-AS partition functions when one uses the $M_{j,\tau}$ schemes designed for strong coupling are larger. With the (2 : 2) and (1 : 3) schemes, the ratios of the MS-AS to the MS-RS partition functions are 1.33–1.41 from 400 K to 600 K. The deviations are a consequence of the MS-RS scheme being designed as an affordable approximation to the nearly separable MS-AS method. The levels of agreement between the results of the methods confirm the principle behind the design of the reference-structure method.

Because the MS-ASCB method uses the most information about the potential energy surface, it is expected—in the absence of cancellation of errors—to be the most accurate of the methods presented here. The good agreement observed between the results of the MS-AS and MS-ASCB methods suggests that the simpler MS-AS method is capable of providing reliable results. Finally, the comparable accuracy and reduced cost of the MS-RS method make it particularly well suited for accounting for the torsional anharmonicity of systems with a large numbers of torsions.

V. Concluding remarks

In this article, we proposed a new family of approximations called multi-structural methods for including torsional anharmonicity in thermodynamics calculations. These methods can be applied to molecules with multiple torsions coupled with each other or with other low-frequency vibrational modes. A key feature of the methods is the use of internal coordinates to correct for torsional anharmonicity so that assigning a torsion to a specific normal mode is not required in the multi-structural methods. These methods only require geometry optimizations and frequency calculations (*i.e.*, no scans) and are easily implemented. The MS-AS

method is designed to be as accurate as possible without requiring any information about the conformational barriers or the paths connecting the structures. We recommend the MS-AS method based on its good balance between computational cost, simplicity, and accuracy. The simpler MS-RS method, which is an approximation to the MS-AS method for the cases of nearly separable torsions, is also found to perform well in our tests and is recommended for large systems when the cost and effort of the MS-AS method are not affordable or not justified.

A portable and documented FORTRAN package for computing the MS partition functions conveniently is under preparation, and it will be made available at no cost when it is ready.

Appendix A

Glossary of acronyms

CHO	Classical harmonic oscillator
CM	Classical mechanical
CO	An interpolation scheme for torsional anharmonicity based on Pitzer's approximation for the moment of inertia along the curvilinear torsion (denoted C for curvilinear) and on the torsional frequency ω (denoted O for omega).
FR	Free rotor
GA	Group additivity (method)
HO	Harmonic oscillator
MS	Multi-structural
MS-AS	Multi-structural method including all structures
MS-AS(I)	MS-AS method with approximation I
MS-AS(M)	MS-AS method with approximation M
MS-AS(S)	MS-AS method with approximation S
MS-ASCB	Multi-structural method including all structures and conformational barrier heights
MS-HO	Multi-structural harmonic-oscillator method
MS-RS	Multi-structural method using a reference-structure treatment involving the generation of structures by independent torsions
NS	Nearly separable torsions
QHO	Quantum mechanical harmonic oscillator
QM	Quantum mechanical
RC	Reference classical (approximation)
RPG	Reference Pitzer–Gwinn (approximation)
SC	Strongly coupled (torsions)
SRC	Segmented reference classical (approximation)
SRPG	Segmented reference Pitzer–Gwinn (approximation)
TES	Torsional eigenvalue summation, that is, evaluation of torsional partition functions by summing Boltzmann factors based on numerically computed eigenvalues of separable torsions
ZPE	Zero-point energy

Appendix B

The thermodynamic functions for the internal (*i.e.*, neglecting translational contributions) free energy, average energy, and entropy are

$$G = -\ln(Q)/\beta \tag{B1}$$

$$E = -\frac{\partial \ln(Q)}{\partial \beta} \tag{B2}$$

$$S = k_{\mathrm{B}} \ln Q - \frac{1}{T}\left(\frac{\partial \ln Q}{\partial \beta}\right)_V \tag{B3}$$

If we use the classical expression for the rotational partition function

$$Q_{\mathrm{rot},j} = \frac{\sqrt{\pi}}{\sigma_{\mathrm{rot},j}}\left(\frac{2}{\hbar^2\beta}\right)^{3/2}\sqrt{I_A I_B I_C} \tag{B4}$$

where I_{A}, I_{B}, and I_{C} are the principal moments of inertia, the partial derivative of the MS-AS partition function with respect to β is

$$\begin{aligned}
&-\frac{\partial}{\partial\beta}\ln(Q_{\text{con-rovib}}^{\text{MS-AS}}) \\
&= \frac{1}{Q_{\text{con-rovib}}^{\text{MS-AS}}}\sum_{j=1}^{J}\left\{e^{-\beta U_j}Q_{\mathrm{rot},j}Q_j^{\mathrm{HO}}Z_j\prod_{\tau=1}^{t}f_{j,\tau}\left(\frac{3}{2\beta}+U_j\right)\right. \\
&+\sum_{m=1}^{F}\frac{\hbar\omega_{j,m}}{2}\frac{1+e^{-\beta\hbar\omega_{j,m}}}{1-e^{-\beta\hbar\omega_{j,m}}} \\
&-\left(g\frac{(1-Z_j^{\mathrm{int}}Z_j^{\mathrm{coup}})}{2t\sqrt{\beta}Z_j}\left\{\sum_{\tau=1}^{t}\frac{\bar{\omega}_{j,\tau}\sqrt{2\pi I_{j,\tau}}}{M_{j,\tau}}\frac{\mathrm{sech}^2(\bar{\omega}_{j,\tau}\sqrt{2\pi I_{j,\tau}\beta}/M_{j,\tau})}{\tanh(\bar{\omega}_{j,\tau}\sqrt{2\pi I_{j,\tau}\beta}/M_{j,\tau})}\right\}\right) \\
&\left.+\sum_{\tau=1}^{t}\left(\frac{I_{j,\tau}\bar{\omega}_{j,\tau}^2}{M_{j,\tau}^2}-\frac{1}{2\beta}-\frac{I_{j,\tau}\bar{\omega}_{j,\tau}^2}{M_{j,\tau}^2}\frac{I_1(\beta I_{j,\tau}\bar{\omega}_{j,\tau}^2/M_{j,\tau}^2)}{I_0(\beta I_{j,\tau}\bar{\omega}_{j,\tau}^2/M_{j,\tau}^2)}\right)\right\}
\end{aligned} \tag{B5}$$

Note that the ZPE corresponding to the MS-AS partition function is the same as for the MS-HO method, *i.e.*,

$$E_0^{\text{MS-HO}} = \min_j\{E_{j,0}^{\mathrm{HO}} + U_j\} \tag{B6}$$

where $E_{j,0}^{\mathrm{HO}}$ is the harmonic oscillator zero-point energy of structure j with the zero of energy at its local minimum, and which is given by

$$E_{j,0}^{\mathrm{HO}} = \frac{\hbar}{2}\sum_{m=1}^{F}\omega_{j,m} \tag{B7}$$

Appendix C

In this appendix, three alternative versions of the MS-AS method are presented; they are labeled MS-AS(I), MS-AS(S), and MS-AS(M).

MS-AS(I)

An alternative method similar to prior work[13,14] would be

$$f_{j,\tau}^{(\mathrm{I})} = \frac{\sigma_\tau}{M_{j,\tau}} \frac{q_{\tau;j}^{\mathrm{MC\text{-}HO}}}{q_{j,\tau}^{\mathrm{QHO}}} \tanh\left(\frac{q_{j,\tau}^{\mathrm{FR}}}{q_{\tau;j}^{\mathrm{MC\text{-}I}}}\right) \qquad \text{(C1)}$$

where

$$q_{\tau;j}^{\mathrm{MC\text{-}I}} = \sum_{i=1}^{M_{j,\tau}/\sigma_\tau} \exp(-\beta[U_i - U_j]) q_{i,\tau}^{\mathrm{CHO}} \qquad \text{(C2)}$$

$$q_{\tau;j}^{\mathrm{MC-HO}} = \sum_{i=1}^{M_{j,\tau}/\sigma_\tau} \exp(-\beta[U_i - U_j]) q_{i\tau}^{\mathrm{HO}} \qquad \text{(C3)}$$

and where the sums in eqn (C2) and (C3) runs over only the minima connected to minimum j by torsion τ. However, in practice this scheme may be difficult to apply because it requires the user to identify which minima are generated by a specified torsion. Therefore, we will instead consider two simple approaches that do not have this requirement.

MS-AS(S)

A simple conformation-specific interpolation function similar to those advocated previously[13] may be used to obtain correct high and low temperature limits, yielding

$$f_{j,\tau}^{(\mathrm{S})} = \tanh\left(\frac{\frac{\sigma_\tau}{M_{j,\tau}} q_{j,\tau}^{\mathrm{FR}}}{q_{j,\tau}^{\mathrm{CHO}}}\right) \qquad \text{(C4)}$$

MS-AS(M)

An alternative approach would be to seek a correction factor of the form

$$f_{j,\tau}^{(\mathrm{M})} = \tanh\left(\frac{N' q_{j,\tau}^{\mathrm{FR}}}{q_{\tau}^{\mathrm{MS\text{-}CHO}}}\right) \qquad \text{(C5)}$$

where

$$q_{\tau}^{\mathrm{MS-CHO}} = \sum_{j=1}^{J} \exp(-\beta U_j) q_{j,\tau}^{\mathrm{CHO}} \qquad \text{(C6)}$$

and where N' is chosen to get a reasonable high-temperature limit. This may be accomplished by choosing

$$N' = N^{1/t} \qquad \text{(C7)}$$

where

$$N = \frac{\prod_{\tau=1}^{t} \sum_{j=1}^{J} e^{-\beta U_j} q_{j,\tau}^{\mathrm{CHO}}}{\sum_{j=1}^{J} e^{-\beta U_j} \prod_{\tau=1}^{t} q_{j,\tau}^{\mathrm{CHO}}} = \frac{\prod_{\tau=1}^{t} q_{\tau}^{\mathrm{MS-CHO}}}{\sum_{j=1}^{J} e^{-\beta U_j} \prod_{\tau=1}^{t} q_{j,\tau}^{\mathrm{CHO}}} \qquad \text{(C8)}$$

Results

Partition functions calculated by the last two alternative versions for the two 1-D models and for ethanol and 1-pentyl radical are tabulated in Table S1 to S5 of the electronic supporting information. Fig. A1–A4 plot the ratio of the partition function calculated by the multi-structural approximations to that calculated by the multi-structural HO approximation for the 1-D models, ethanol, and 1-pentyl radical. Unlike the MS-AS and MS-ASCB results, the

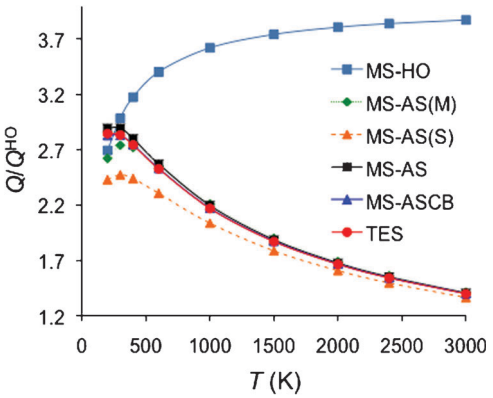

Fig. A1 Ratios of the partition function of the 1-D potential of eqn (48) calculated by multi-structural methods or the TES method to that calculated by the single-structural HO approximation at the global minimum.

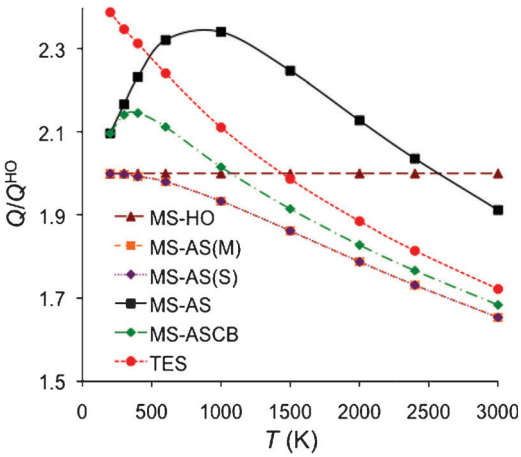

Fig. A2 Ratios of partition functions of the 1-D potential of H_2O_2 calculated by multi-structural methods or the TES method to those calculated by the single-structural HO approximation at the global minimum.

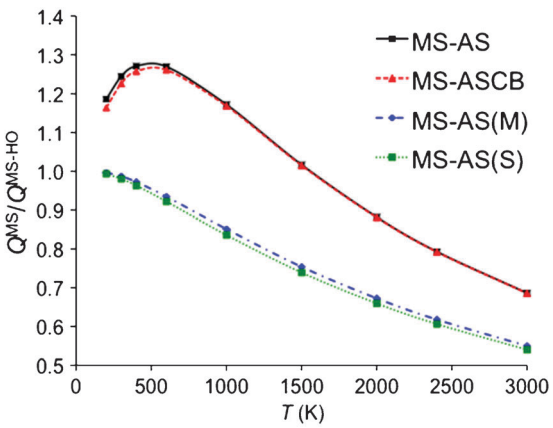

Fig. A3 Ratio of the partition functions for ethanol calculated by multi-structural methods including torsional anharmonicity to those calculated by the MS-HO approximation at the global minimum.

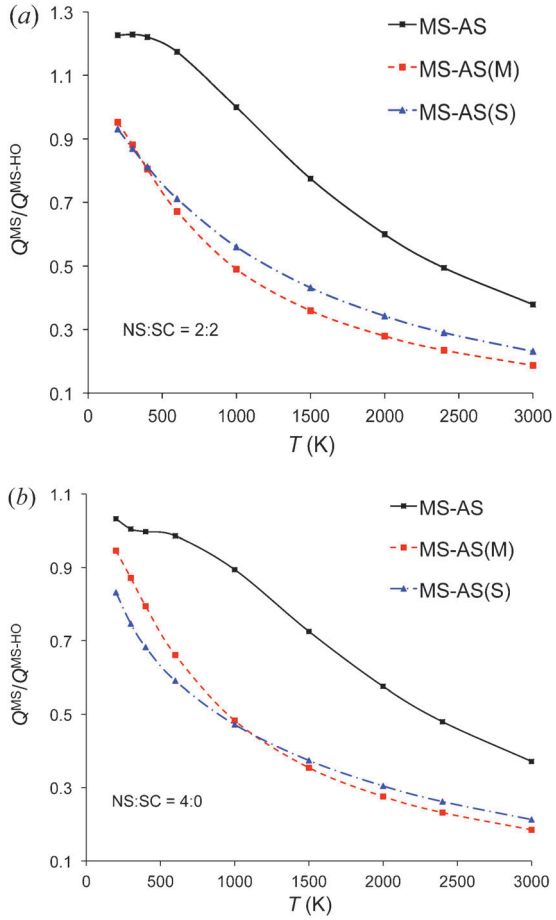

Fig. A4 Ratios of partition functions for 1-pentyl radical calculated by the multi-structural methods including torsional anharmonicity to those calculated by the MS-HO approximation. Note the calculations used $M_{j,\tau}$ parameters predicted by the scheme NS : SC = 2 : 2 for (a) and NS : SC = 4 : 0 for (b).

MS-AS(S) and MS-AS(M) results are always below the MS-HO result. They agree well with the MS-HO results at low T and with the MS-AS and MS-ASCB results in the high-temperature limit. The MS-AS(M) scheme leads to every torsion approaching the free-rotor limit at the same rate, which is unnecessarily restrictive. While the MS-AS(S) scheme performs adequately, the MS-AS scheme has the potential to lead to superior results at intermediate temperatures; as a consequence, these alternative schemes are not recommended for future use.

Appendix D

Previous papers[13,14] presented several methods that use normal mode substitution treat each torsion separately by using various schemes, *e.g.*, CO, RPG, SPRG, and TES, and treat the other vibrational degrees of freedom based on information from one structure. Because these methods all need to identify each torsion with one of the normal modes, they are not applicable to the molecules considered here. For the systems studied in this paper, 1-pentyl radical and 1-butanol have torsional modes that are coupled with each other and with low frequency bending modes, and in ethanol the two torsional motions are completely mixed in the two lowest normal modes. Table 14 illustrates the use of the CO, SRPG, RPG, and TES approximations for ethanol where the calculations are performed by assigning the lowest normal mode frequency to C–C torsion and the second lowest normal mode frequency to C–O torsion. The normal-mode torsional frequencies and internal moment of inertial used in the CO method are calculated for each conformer instead of using an averaged value as advocated previously,[13] and the RPG method implemented here uses an effective barrier height that is taken as the average of the left and right barriers rather than that obtained using eqn (13). The TES values were obtained by fitting 40 points along each torsion to a 10-term Fourier cosine series.

Table 14 Partition function of ethanol calculated by various approximations[a]

T/K	CO	SRPG	RPG	TES
100	4.30E-104	5.77E-104	6.80E-104	7.03E-104
150	5.64E-68	7.79E-68	8.74E-68	8.54E-68
200	8.38E-50	1.16E-49	1.29E-49	1.25E-49
300	1.99E-31	2.77E-31	3.02E-31	2.95E-31
400	4.78E-22	6.71E-22	7.25E-22	7.13E-22
600	2.82E-12	3.96E-12	4.21E-12	4.22E-12
1000	1.40E-03	1.94E-03	2.02E-03	2.05E-03
1500	2.74E + 02	3.66E + 02	3.77E + 02	3.84E + 02
2000	5.26E + 05	6.76E + 05	6.93E + 05	7.07E + 05
2400	4.72E + 07	5.97E + 07	6.08E + 07	6.18E + 07
3000	9.56E + 09	1.17E + 10	1.19E + 10	1.21E + 10
4000	7.14E + 12	8.46E + 12	8.54E + 12	8.67E + 12
7000	1.87E + 18	2.09E + 18	2.09E + 18	2.12E + 18
50 000	6.04E + 36	6.14E + 36	6.14E + 36	6.17E + 36

[a] All the frequencies in the CO, SRPG, RPG calculations are scaled by a factor $\lambda = 0.970$ for M06-2X/6-311 + G(2df,2p) method,[69] and λ^2 is used to scale the 1-D potentials used in TES calculations.

Comparison of the results in Table 14 to the MS-ASCB results in Table 7 shows that for 400 K and above there is excellent agreement of the TES results, very good agreement of the SRPG results, and good agreement of RPG results; the agreement deteriorate at lower temperatures. However, there is no straightforward way to assign the torsions to individual normal modes for 1-butanol or 1-pentyl radical, and so these methods are not generally applicable.

Acknowledgements

This work was supported in part by the US Department of Energy, Office of Science, Office of Basic Energy Sciences, under Grant No. DE-FG02-86ER13579, and as part of the Combustion Energy Frontier Research Center under Award Number DE-SC0001198.

References

1 *Quantum Mechanics and Path Integrals*, R. P. Feynman and A. R. Hibbs, McGraw-Hill, New York, 1965.
2 *Statistical Mechanics*, R. P. Feynman, Benjamin, Reading, MA, 1972.
3 V. A. Lynch, S. L. Mielke and D. G. Truhlar, *J. Chem. Phys.*, 2004, **121**, 5148.

4 V. A. Lynch, S. L. Mielke and D. G. Truhlar, *J. Phys. Chem. A*, 2005, **109**, 10092; 2006, **110**, 5965(E).
5 S. Chempath, C. Predescu and A. T. Bell, *J. Chem. Phys.*, 2006, **124**, 234101.
6 D. R. Herschbach, *J. Chem. Phys.*, 1959, **31**, 91.
7 D. G. Truhlar, *J. Comput. Chem.*, 1991, **12**, 266.
8 J. Gang, M. J. Pilling and S. H. Robertson, *J. Chem. Soc., Faraday Trans.*, 1996, **92**, 3509.
9 A. L. L. East and L. Radom, *J. Chem. Phys.*, 1997, **106**, 6655.
10 R. B. McClurg, R. C. Flagan and W. A. Goddard, III, *J. Chem. Phys.*, 1997, **106**, 6675; 1999, **111**, 7165(E).
11 W. Witschel and C. Hartwigsen, *Chem. Phys. Lett.*, 1997, **273**, 304.
12 P. Y. Ayala and H. B. Schlegel, *J. Chem. Phys.*, 1998, **108**, 2314.
13 Y.-Y. Chuang and D. G. Truhlar, *J. Chem. Phys.*, 2000, **112**, 1221; 2004, **121**, 7036(E); 2006, **124**, 179903(E).
14 B. A. Ellingson, V. A. Lynch, S. L. Mielke and D. G. Truhlar, *J. Chem. Phys.*, 2006, **125**, 084305.
15 A. C. P. Bitencourt, M. Ragni, G. S. Maciel, V. Aquilanti and F. V. Prudente, *J. Chem. Phys.*, 2008, **129**, 154316.
16 S. Sharma, S. Raman and W. H. Green, *J. Phys. Chem. A*, 2010, **114**, 5689.
17 D. Gruzman, A. Karton and J. M. L. Martin, *J. Phys. Chem. A*, 2009, **113**, 11974.
18 T. H. Lay, L. N. Krasnoperov, C. A. Venanzi, J. W. Bozzelli and N. V. Shokhirev, *J. Phys. Chem.*, 1996, **100**, 8240.
19 T. Yamada, T. H. Lay and J. W. Bozzelli, *J. Phys. Chem. A*, 1998, **102**, 7286.
20 T. Yamada, J. W. Bozzelli and R. J. Berry, *J. Phys. Chem. A*, 1999, **103**, 5602.
21 K. S. Pitzer and W. D. Gwinn, *J. Chem. Phys.*, 1942, **10**, 428.
22 B. M. Wong and W. H. Green, *Mol. Phys.*, 2005, **103**, 1027.
23 T. F. Miller, III and D. C. Clary, *J. Chem. Phys.*, 2002, **116**, 8262.
24 V. Van Speybroeck, D. V. Neck and M. Waroquier, *J. Phys. Chem. A*, 2002, **106**, 8945.
25 P. Vansteenkiste, D. Van Neck, V. Van Speybroeck and M. Waroquier, *J. Chem. Phys.*, 2006, **124**, 044314.
26 *Statistical Mechanics*, D. A. McQuarrie, Harper & Row, New York, 1973.
27 T. F. Miller, III and D. C. Clary, *Mol. Phys.*, 2005, **103**, 1573.
28 M. Tafipolsky and R. Schmid, *J. Comput. Chem.*, 2005, **26**, 1579.
29 Y. K. Sturdy and D. C. Clary, *Phys. Chem. Chem. Phys.*, 2007, **9**, 2397.
30 S. W. Benson, *Thermochemical Kinetics*, Wiley-Interscience, New York, 2nd edn, 1976.
31 H. E. O'Neal and S. W. Benson, *Int. J. Chem. Kinet.*, 1969, **1**, 221.
32 H. E. O'Neal and S. W. Benson, in *Free Radicals*, ed. J. H. Koshi, Wiley, New York, 1973, p. 275.
33 N. Cohen, *J. Phys. Chem.*, 1992, **96**, 9052.
34 T. H. Lay, J. W. Bozzelli, A. M. Dean and E. R. Ritter, *J. Phys. Chem.*, 1995, **99**, 14514.
35 K. K. Irikura, in *Computational Thermochemistry*, ed. K. K. Irikura and D. J. Frurip, ACS Symposium Series, 1998, vol. 677, p. 402.
36 V. Van Speybroeck, R. Ganib and R. J. Meier, *Chem. Soc. Rev.*, 2010, **39**, 1764.
37 K. S. Pitzer, *J. Chem. Phys.*, 1940, **8**, 711.
38 W. J. Taylor, *J. Chem. Phys.*, 1948, **16**, 257.
39 P. J. Flory and R. L. Jernigan, *J. Chem. Phys.*, 1965, **42**, 3509.
40 R. A. Scott and H. A. Scheraga, *J. Chem. Phys.*, 1966, **44**, 3054.
41 R. Janoschek and J. Kalcher, *Z. Anorg. Allg. Chem.*, 2002, **628**, 2724.
42 G. L. Dirichlet, *J. Reine Angew. Math.*, 1850, **40**, 209.
43 G. Voronoi, *J. Reine Angew. Math.*, 1907, **133**, 97.
44 F. Aurenhammer, *ACM Computing Surveys*, 1991, **23**, 345.
45 G. Katzer and A. F. Sax, *J. Comput. Chem.*, 2005, **26**, 1438.
46 K. S. Pitzer, *J. Chem. Phys.*, 1946, **14**, 239.
47 J. E. Kilpatrick and K. S. Pitzer, *J. Chem. Phys.*, 1949, **17**, 1064.
48 T. Miyazawa and K. Fukushima, *J. Mol. Spectrosc.*, 1965, **15**, 308.
49 H. Bonadeo, E. D'Alessio and E. Silberman, *J. Mol. Spectrosc.*, 1967, **22**, 402.
50 G. Keresztury, A.-Y. Wang and J. R. Durig, *Spectrochim. Acta, Part A*, 1992, **48**, 199.
51 G. Tasi, F. Mizukami, I. Palinko, J. Csontos, W. Gyorffy, P. Nair, K. Maeda, M. Toba, S.-i. Niwa, Y. Kiyozumi and I. Kiricsi, *J. Phys. Chem. A*, 1998, **102**, 7698.
52 D. Bond, *J. Phys. Chem. A*, 2008, **112**, 1656.
53 P. Pulay, *Mol. Phys.*, 1969, **17**, 197.
54 *Molecular Vibrational Spectra and Structure*, G. Fogarasi and P. Pulay, Elsevier, Amsterdam, 1985.
55 C. F. Jackels, Z. Gu and D. G. Truhlar, *J. Chem. Phys.*, 1995, **102**, 3188.
56 K. A. Nguyen, C. F. Jackels and D. G. Truhlar, *J. Chem. Phys.*, 1996, **104**, 6491.
57 Y.-Y. Chuang and D. G. Truhlar, *J. Chem. Phys.*, 1997, **107**, 83.
58 *Molecular Vibrations*, E. B. Wilson, Jr., J. C. Decius and P. C. Cross, McGraw-Hill, New York, 1955.
59 C.-L. Huang, C.-L. Liu, C.-K. Ni and J. T. Hougen, *J. Mol. Spectrosc.*, 2005, **233**, 122.
60 V. Hanninen and L. Halonen, *J. Chem. Phys.*, 2007, **126**, 064309.
61 G. Katzer and A. F. Sax, *Chem. Phys. Lett.*, 2003, **368**, 473.
62 K. L. Clarkson, K. Mehlhorn and R. Seidel, *Lect. Notes Comput.Sci.*, 1992, **577**, 463.
63 A program for convex hulls, http://www.netlib.org/voronoi/hull.html.
64 Y. Zhao and D. G. Truhlar, *Theor. Chem. Acc.*, 2008, **120**, 215.
65 B. J. Lynch, P. L. Fast, M. Harris and D. G. Truhlar, *J. Phys. Chem. A*, 2000, **104**, 4811.
66 R. Krishnan, J. S. Binkley, R. Seeger and J. A. Pople, *J. Chem. Phys.*, 1980, **72**, 650.
67 T. Clark, J. Chandrasekhar, G. W. Spitznagel and P. v. R. Schleyer, *J. Comput. Chem.*, 1983, **4**, 294.
68 M. J. Frisch, G. W. Trucks, H. B. Schlegel, G. E. Scuseria, M. A. Robb, J. R. Cheeseman, G. Scalmani, V. Barone, B. Mennucci, G. A. Petersson, H. Nakatsuji, M. Caricato, X. Li, H. P. Hratchian, A. F. Izmaylov, J. Bloino, G. Zheng, J. L. Sonnenberg, M. Hada, M. Ehara, K. Toyota, R. Fukuda, J. Hasegawa, M. Ishida, T. Nakajima, Y. Honda, O. Kitao, H. Nakai, T. Vreven, J. A. Montgomery, Jr., J. E. Peralta, F. Ogliaro, M. Bearpark, J. J. Heyd, E. Brothers, K. N. Kudin, V. N. Staroverov, R. Kobayashi, J. Normand, K. Raghavachari, A. Rendell, J. C. Burant, S. S. Iyengar, J. Tomasi, M. Cossi, N. Rega, N. J. Millam, M. Klene, J. E. Knox, J. B. Cross, V. Bakken, C. Adamo, J. Jaramillo, R. E. Gomperts, O. Stratmann, A. J. Yazyev, R. Austin, C. Cammi, J. W. Pomelli, R. Ochterski, R. L. Martin, K. Morokuma, V. G. Zakrzewski, G. A. Voth, P. Salvador, J. J. Dannenberg, S. Dapprich, A. D. Daniels, O. Farkas, J. B. Foresman, J. V. Ortiz, J. Cioslowski and D. J. Fox, *GAUSSIAN 09*, Gaussian Inc., Wallingford CT, Revision A.02, 2009.
69 I. M. Alecu, J. Zheng, Y. Zhao and D. G. Truhlar, *J. Chem. Theory Comput.*, 2010, **6**, 2872.
70 S. W. Benson, F. R. Cruickshank, D. M. Golden, G. R. Haugen, H. E. O'Neal, A. S. Rodgers, R. Shaw and R. Walsh, *Chem. Rev.*, 1969, **69**, 279.
71 J. Koput, S. Carter and N. C. Handy, *J. Phys. Chem. A*, 1998, **102**, 6325.
72 K. Ohno, H. Yoshida, H. Watanabe, T. Fujita and H. Matsuura, *J. Phys. Chem.*, 1994, **98**, 6924.
73 J. Moc, J. M. Simmie and H. J. Curran, *J. Mol. Struct.*, 2009, **928**, 149.
74 L. V. Gurvich, I. V. Veyts and C. B. Alcock, *Thermodynamic Properties of Individual Substances*, Hemisphere Pub. Co., New York, 4th edn, 1989.
75 J. F. Counsell, J. L. Hales and J. F. Martin, *Trans. Faraday Soc.*, 1965, **61**, 1869.
76 E. Hirota, *J. Chem. Phys.*, 1958, **28**, 839.
77 R. M. Lees, *J. Chem. Phys.*, 1973, **59**, 2690.
78 R. Meyer, *J. Mol. Spectrosc.*, 1979, **76**, 266.
79 G. A. Guirgis, J. B. A. Barton and J. R. Durig, *J. Chem. Phys.*, 1983, **79**, 5918.
80 J. A. Kunc, *Mol. Phys.*, 2003, **101**, 413.
81 C. Y. Lin, E. I. Izgorodina and M. L. Coote, *J. Phys. Chem. A*, 2008, **112**, 1956.